

UNCLASSIFIED

AD 407990

DEFENSE DOCUMENTATION CENTER

FOR

SCIENTIFIC AND TECHNICAL INFORMATION

CAMERON STATION, ALEXANDRIA, VIRGINIA



UNCLASSIFIED

NOTICE: When government or other drawings, specifications or other data are used for any purpose other than in connection with a definitely related government procurement operation, the U. S. Government thereby incurs no responsibility, nor any obligation whatsoever; and the fact that the Government may have formulated, furnished, or in any way supplied the said drawings, specifications, or other data is not to be regarded by implication or otherwise as in any manner licensing the holder or any other person or corporation, or conveying any rights or permission to manufacture, use or sell any patented invention that may in any way be related thereto.

AD NO. 07990

DDC FILE COPY

407990

(5) 551 500

63-4-2

0

A FEASIBILITY STUDY OF AN OPTICAL
RANGING DEVICE FOR SPACE VEHICLES

by

Alfred J. Hallisey

and

Albert E. Johansen

S. M.

Course XVI

June 1963



\$ 8.10

(5) 554 500

(4) D#8.10

(6) A FEASIBILITY STUDY OF AN OPTICAL
RANGING DEVICE FOR SPACE VEHICLES

(7) MA

(8) by

(9) MA

ALFRED J. HALLISEY

(10) MA

B. S., U. S. MILITARY ACADEMY, 1956

and

(11) MA

ALBERT E. JOHANSEN

B. S., U. S. AIR FORCE ACADEMY, 1961

(12) MA

SUBMITTED IN PARTIAL FULFILLMENT OF THE

(13) MA

REQUIREMENTS FOR THE DEGREE OF

MASTER OF SCIENCE

(14) MA

at the

(15) MA

MASSACHUSETTS INSTITUTE OF TECHNOLOGY

June, 1963

(16) MA

Signatures of Authors

Alfred J. Hallisey

(17) MA

their

Albert E. Johansen

(18) MA

Certified by

Karel E. Degler

(19) MA

Accepted by

Chairman, Departmental
Graduate Committee

A FEASIBILITY STUDY OF AN OPTICAL
RANGING DEVICE FOR SPACE VEHICLES

by

Alfred J. Hallisey

Albert E. Johansen

Submitted to the Department of Aeronautics and Astronautics
on May 17, 1963, in partial fulfillment of the requirements of the
degree of Master of Science.

ABSTRACT

A theoretical investigation of light intensities and wave shape characteristics necessary for precise ranging in the cis-lunar environment was carried out. Preliminary experiments were completed relative to the more critical parameters of ranging. The results of the theoretical and experimental observations led to the conclusion that optical ranging with high intensity, short duration light beacons is indeed feasible. 

In particular, commercially available xenon flash tubes were utilized in combination with high voltages and small capacitances which resulted in fast rise times and high output light intensities. The problem of precise triggering upon command from a receiver-transponder was overcome with a trigger circuit which utilized a combination spark gap and thyratron to provide a high voltage pulse with very little jitter. Several reflector types were investigated and it was determined that a more concentrated source or a diffuse reflector with an extended source would suffice.

The construction and appraisal of various telescope and photosensor combinations, capable of detecting the estimated ranging signal intensities were completed. The use of one of these devices as a transponder to demonstrate its application in triggering a return pulse was investigated. Passive ranging was conducted to demonstrate the ability of some of the system components to perform range measurements with a 1% accuracy.

Thesis Supervisor: Harold E. Edgerton
Professor of Electrical
Measurements

ACKNOWLEDGEMENTS

The authors wish to express their appreciation to the following persons: Prof. H. E. Edgerton and V. E. MacRoberts for their constructive suggestions, Janusz Sciegienny for his interest, enthusiasm, and guidance, Prof. A. C. Hardy, Ken Foster and John Goncz for their technical advice, and the staff of the Optics Division of the MIT Instrumentation Laboratory. Particular thanks are due Thane Kriegel and David Smith for their active participation and most able assistance in the laboratory. Finally, we wish to express sincere appreciation to our wives for their patience and assistance.

The graduate work for which this thesis is a partial requirement was performed while the authors were assigned by the Air Force Institute of Technology for graduate training at the Massachusetts Institute of Technology.

LIST OF SYMBOLS

B_{F_a}	Apparent field brightness at the eye
B_{F_m}	Background brightness of the lunar surface
B_{F_r}	Actual field brightness without optical aids
B_{F_s}	Background brightness equivalent to star field illumination
D_e	Exit pupil diameter of the telescope
D_o	Diameter of the telescope objective lens
D_p	Entrance pupil diameter of the eye
E_a	Apparent illumination received by the eye
E_r	Actual illumination received by the objective lens of the telescope
E_s	Illumination received from star field background
E_t	Threshold illumination of the eye
E_6	Illumination received at the surface of the earth for a 6th magnitude star
M	Magnification of the telescope
T_E	Vertical transmissivity of the earth's atmosphere

v

T_T Transmissivity of the telescope

ω Solid angle of the field of view

LIST OF EQUIPMENT

Oscilloscope, Model 545A, Tektronix, Inc.
 Oscilloscope Camera, Model C-12, Tektronix, Inc.
 High Voltage Power Supply, Model 20HPT5-1, Del Electronics Corp.
 Regulated Power Supply, Model 702A, Beckman Instruments, Inc.
 Laser Power Supply, Model 521, Edgerton, Germeshausen and Grier
 Power Transformer, Model 980494-A, Westinghouse
 Strobetac, Model 1531-A, General Radio Company
 Variac Autotransformer, Model W5MT, General Radio Company
 Special Trigger Circuit, Edgerton, Germeshausen and Grier
 Telescope Elbow Model M17, Eastman Kodak Co.
 3 Power Telescope, Model M-70C, Bulova Watch Co.
 VOM, Model 269, Simpson Electric Co.
 VTVM, Model 1M-10, Heath Company
 Fan, Model B10AJ17, Diehl Manufacturing Co.

Capacitors

<u>Capacitance</u>	<u>Max Voltage</u>	<u>Model Number</u>	<u>Manufacturer</u>
0.5	20KV	Y39085	General Electric
0.25	20KV	X49670	General Electric
0.25	12.5KV	J98727	General Electric
0.10	20KV	V27592	General Electric
0.05	20KV	P15606	Sprague
0.03	16KV	KS8595	General Electric
0.012	20KV	45P5	Sprague
0.01	10KV	P15603	Sprague

CONTENTS

Introduction	1
Chapter I. Theory	3
A. Mission Profile and Background	
Illumination	3
B. Threshold Illumination	9
C. Requirements for Short Duration Flashes	12
D. System Components	20
Chapter II. Experimental Procedures	24
A. High Voltage	24
B. Spark Gaps	27
C. Trigger Circuit	30
D. Photosensitive Devices	34
E. Reflector	37
Chapter III. Experimental Results	38
A. Intensity and Rise Time Measurements	38
B. Jitter	49
C. Reflectors	53
D. Preliminary Ranging	60
Chapter IV. Conclusions and Recommendations	64
Appendix "A". Intensity and Brightness	66
Appendix "B". Tables	68
Table I. Intensity and Rise Time Measurements	69

Table II. Radial Distribution of Luminous Flux in the Horizontal Plane	70
Table III. Distribution of Luminous Flux from Parabolic Reflector	71
References	72

LIST OF FIGURES

1.	Relative Positions of Moon, Earth, and Sun	4
2.	Orbital Parameters	7
3.	Threshold Illumination	10
4.	Parameters of a 3rd Magnitude Star Equivalent Flashing Beacon	15
5.	Stellar Magnitude versus Range for Constant Energy	18
6.	Energy per Flash versus Range for Constant Stellar Magnitude	18
7.	Allowable Error versus Range for 1% Accuracy in Range	19
8.	Power Supplies, Trigger Circuit, and Transponder	25
9.	Close-up of Spark Gap	29
10.	Termination of Trigger Circuit with Spark Gap and Flash Tube	31
11.	First Stage of Trigger Circuit	32
12.	Close-up of Trigger Circuit	33
13.	Transponder	34
14.	Photomultiplier Circuit for use with 931-A or 1P21	36
15.	Early Jitter Detection	39
16.	Intensity Waveform Photographs at 20 KV with FX-42 Flashlamp	40
17.	Current Waveforms at 20 KV for FX-42 Circuit	42
18.	Peak Intensity versus Capacitance for Different Tube Voltages	43
19.	Peak Intensity versus Tube Voltage for Different Capacitances	44

20.	Peak Intensity versus Input Energy for Different Capacitances	45
21.	Output Energy versus Input Energy for Different tube voltages.	46
22.	Rise Time versus capacitance for Different Tube Voltages	48
23.	Rise Time versus Tube Voltage for Different Capacitances	48
24.	First Jitter Measurement at High Voltage	49
25.	Later Jitter Measurement	52
26.	Expanded View of Fig. 25.	52
27.	Luminosity Pattern of FX-42 for an Indicated Uniform Surface Illumination of 100,000 Lumens per feet ² .	54
28.	Reflector Type #1	56
29.	Reflector Type #2	57
30.	Reflector Type #3	58
31	Ranging to Fire Escape	61
32.	Time Delay and Jitter in Assembly #2	62
33.	Preliminary Ranging	62

INTRODUCTION

A particularly critical problem in manned space flight is accurate range determination during orbital rendezvous. This problem becomes even more critical when only on-board equipment may be used as in the lunar orbital rendezvous phase of the Apollo mission for which primary ranging information will be obtained from on-board radar. In the interest of crew safety, it is desirable to have a back-up method of ranging in the event that the primary radar malfunctions.

In particular, the Command Module (CM/SM) will be in a 100 nautical mile circular orbit from which the Lunar Excursion Module (LEM) will descend to the lunar surface in the approximate plane of the parking orbit. During the lunar rendezvous phase, the CM/SM will first be visible on the horizon at a range of 445 nautical miles. Lunar lift-off will occur when the Command Module is near the LEM's zenith, or at a range of 100 NM. Each vehicle will carry a high intensity xenon "flashlamp to aid in visual acquisition and docking. It is the purpose of this thesis to consider the feasibility of using these flashing light sources as part of a secondary ranging scheme.

Ranging could be accomplished by measuring the total elapsed time between the initial flash at the LEM and the return of a subsequent flash from the CM. An optical transponder on board the CM would trigger its beacon upon receipt of the LEM's flash. The inherent time delay of the transponder would be subtracted from the total elapsed time. Ideally, one-half of this figure represents the

travel time for each light pulse between the vehicles. When multiplied by the speed of light, this determines the range.

As the LEM approaches the Command Module, more accurate ranging information must be determined at more frequent intervals in order to affect a precise docking maneuver. During this closure, the decreasing energy requirement per flash permits a more rapid flash rate without an increase in power consumption.

CHAPTER I

THEORY

A. MISSION PROFILE AND BACKGROUND ILLUMINATION.

Possible landing sites near the lunar equator have been chosen that will be on the dark half of the lunar surface close to the terminator, or the line between the shadowed and sunlit hemispheres. Due to the slow rotation of the moon, the terminator will not move very far across the surface of the moon during the period of exploration.

The relative positions of the sun, moon and earth at the time of exploration of and ascent from the lunar surface will be such that all of the ranging information needed to achieve rendezvous will be obtained while the exploratory vehicles are within the umbra of the moon.

Fig. 1 shows these relative positions at the time of lift-off of the LEM, looking down on the axis of rotation of the moon. This configuration shows that the only significant illumination for an orbiting vehicle observing the lunar surface is the reflected light from a "half earth."

Because of the large size of the earth when viewed from the moon and its greater albedo (0.39 versus 0.07 for the moon), the illumination received at the surface of the moon from a full earth is approximately 100 times that from a full moon measured at the earth's surface.¹ The illumination incident on the moon by a full earth is, in fact, 7.8×10^{-3} lumen-cm⁻².² The surface brightness of the moon illuminated by only half the earth's light is 1.77×10^{-5} candle-cm⁻² if

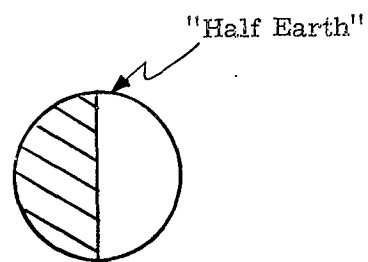
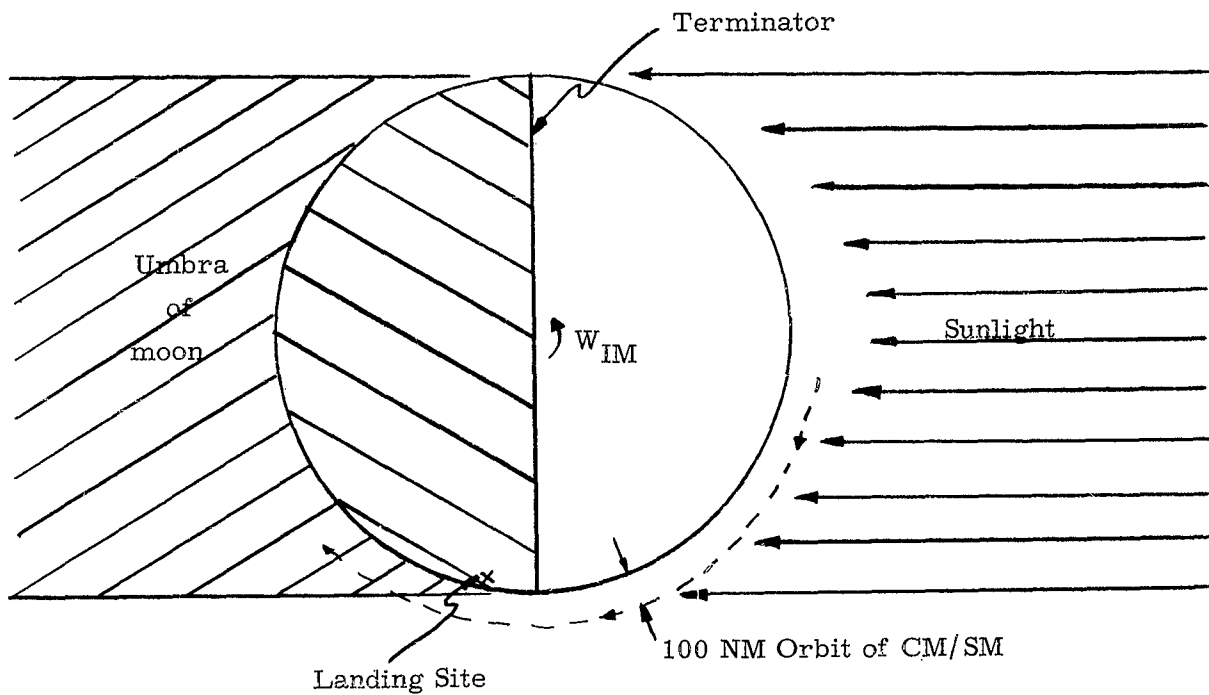


Fig. 1. Relative Positions of Moon, Earth, and Sun

it is viewed from the same direction as the incident light (See APPENDIX A). These figures were computed on the basis of the average distance of the earth from the moon and the average brightness of the moon. The latter figure represents the background illumination seen by an orbiting vehicle viewing a spot on the lunar surface.

Both the LEM and the CM/SM will have viewing telescopes with alternate 3X and 1X magnitudes. In the 3X mode, the field of view of the telescope occupies a solid angle of 100π square degrees, or a cone with an apex angle of 20° . At the expected time of appearance of the CM/SM above the horizon in its passage when the LEM's ascent and rendezvous are to be undertaken, the principal axis of the viewing telescope is constrained to point 10° above the horizon in the plane of the CM/SM's orbit. The direction of the telescope would be "fixed" during each observation sequence by coupling to an inertial platform so that the background star field is invariant while the CM/SM passes through the field of view.

For the case of the LEM sighting the CM/SM, it is reasonable to assume that the presence of many other brighter light sources in the field of view would raise the threshold of visibility of a dark-adapted eye for a single point light source. The brightest star field of view encompassed by the 20° cone angle of the 3X telescope is the 100π square degree section of the celestial sphere in the center of the constellation of Orion. A background brightness level equal to the illumination received from all the stars in that sector might be used to determine the poorest threshold condition to be expected when viewing the night sky. That 100π square degree sector of the

constellation of Orion contains:

<u>No. of Stars</u>	<u>Magnitude</u>	<u>Equivalent Number 6th Magnitude Stars</u>
1	1st	100.0
4	2nd	160.0
2	3rd	31.6
2	4th	12.6
1	5th	<u>2.5</u> <u>306.</u>

The total illumination received is thus equal to that from 306 6th magnitude stars viewed outside the atmosphere, or:

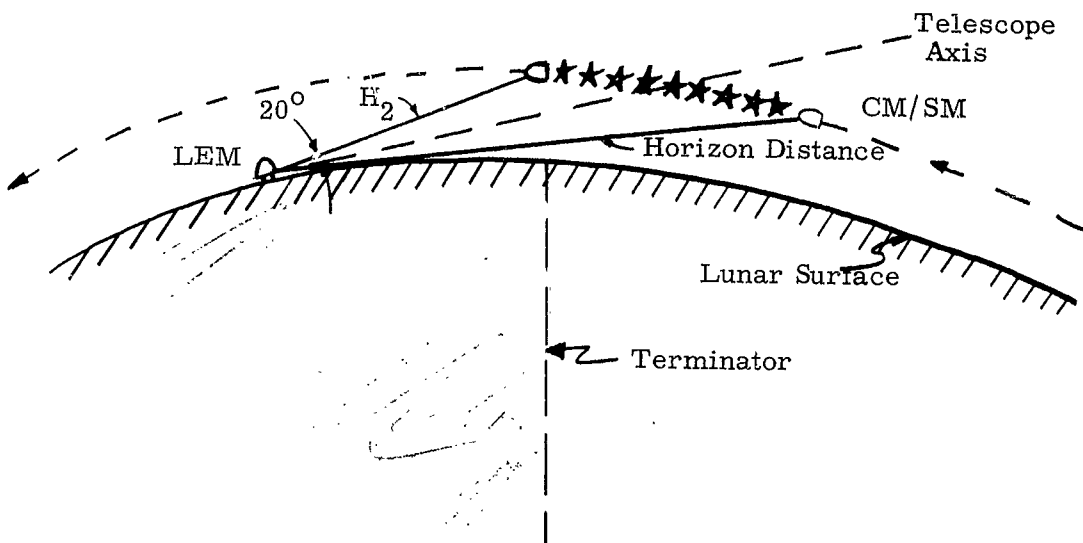
$$E_S = \frac{306 E_6}{T_E} = \frac{306 \times 8.3 \times 10^{-13}}{0.85} = 2.99 \times 10^{-10} \text{ lumen-cm}^{-2}.$$

The equivalent background field illumination is then computed as:

$$B_{FS} = \frac{E_S}{\omega} = \frac{2.99 \times 10^{-10}}{0.0954} = 3.14 \times 10^{-9} \text{ candle-cm}^{-2}$$

Fig. 2 shows the relative positions of the vehicles during the first observation sequence. Some of the pertinent information concerning the passage of the CM/SM in its orbit across the field of view is also contained in this figure. To the observer on the LEM, the sequence of flashes would appear first very faint and close together near the horizon and gradually increase in brightness and angular interval as they move up through the field of view.

Once the LEM has acquired the orbiting vehicle, it will direct its flash at the CM/SM. When the CM/SM has acquired the LEM, a signal will be necessary to announce this to the LEM. This signal



$$(GM)_m = 1.73 \times 10^{14} \text{ ft}^3 \cdot \text{sec}^{-2}$$

$$R_m = 938 \text{ NM}$$

$$R_1 = 1038 \text{ NM}$$

$$\phi_1 = \cos^{-1}(938/1038) = 25.2^\circ$$

$$\phi_2 = 180^\circ - 110^\circ - \sin^{-1} \left[\frac{938(\sin 110^\circ)}{1038} \right]$$

$$\phi_2 = 11.9^\circ$$

Orbital Velocity of CM/SM:

$$v = \left(\frac{GM}{R_m} \right)^{1/2} = 5240 \text{ ft/sec}^{-1}$$

$$W_{IM} = \frac{v}{R_m} = \frac{5240}{(1038)(6080)} = 8.3 \times 10^{-4} \text{ rad/sec}^{-1}$$

Period of Orbit:

$$P = \frac{2\pi}{W_{IM}} = 126 \text{ Minutes}$$

Horizon Distance:

$$H = \sqrt{(1038)^2 - (938)^2} = 445 \text{ NM}$$

Time CM/SM Remains

in Field of View:

$$T_t = \frac{\phi_1 - \phi_2}{57.3 W_{IM}} = 4.67 \text{ Min.}$$

$$H_2 = \frac{R_1}{\sin 110^\circ} \sin \phi_2$$

$$H_2 = 227 \text{ NM}$$

Fig. 2. Orbital Parameters

would immediately precede the change from active flashing to the ranging mode on the CM/SM, after which time the CM/SM's transponder alone would activate its light source. A suggested signal might be to terminate the active flashing on the CM/SM for a specified interval of time before switching to the ranging mode.

Each time the CM/SM has passed entirely across the field of view of the LEM's telescope, the axis of the telescope will be realigned to view the next 20° sector of the orbit. When the sector viewed includes the zenith, the 1X telescope will be utilized for the ascent and rendezvous phase.

B. THRESHOLD ILLUMINATION

The level of intensity of illumination required for detection of a steady achromatic point light source by the naked eye is commonly known as the threshold illumination and is a function of the level of the background brightness. Many noted scholars including Tiffany, Blackwell, Knoll, Tousey, Beard, Green and Hecht have attempted to develop empirical equations and graphical charts that could explain this phenomenon.⁴ The results of many experiments have been recorded and from the data collected a composite plot of the threshold illumination versus background brightness has been constructed. This is shown on Fig. 3 and represents a weighted average of the findings described above as they conform to the observations of Russell.³ This figure includes the expected limits of background brightness of the two different fields of view during the ascent and rendezvous phase of the Apollo mission.

The maximum background brightness (B_{F_a}) that would be observed through the telescope on the LEM must be computed by an empirical telescope equation:²

$$B_{F_a} = T \left(\frac{D_e}{D_p} \right)^2 B_{F_r} = T \left(\frac{D_o}{D_p M} \right)^2 B_{F_s}$$

$$B_{F_a} = 0.25 \left(\frac{1.27}{0.7 \times 3.0} \right)^2 (3.14 \times 10^{-9}) = 2.87 \times 10^{-10} \text{ candle-cm}^{-2}$$

From Fig. 3, the threshold illumination of a steady point source is approximately 1.0×10^{-13} lumen-cm⁻². This value must then be used to compute the intensity of illumination required on the objective lens,

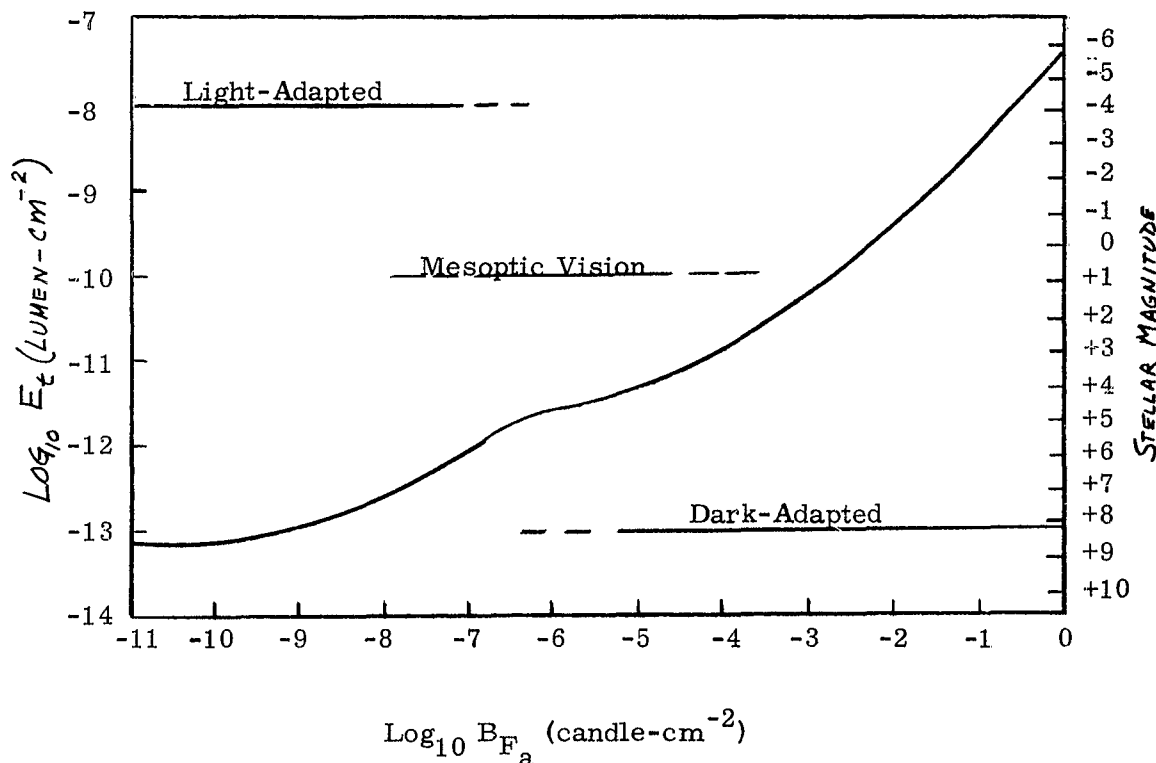


Fig. 3. - Adapted curve of threshold illumination from a fixed achromatic point source, detectable with a practical certainty by the normal human eye, as a function of background brightness.

(E_r), by another telescope equation where $E_t = E_a^2$

$$E_r = \frac{1}{T_T} \left(\frac{D_p}{D_o} \right)^2 \quad E_a = \frac{1}{0.25} \left(\frac{0.7}{1.27} \right)^2 (1.0 \times 10^{-13})$$

$$E_r = 1.21 \times 10^{-13} \text{ lumen-cm}^{-2}$$

This means that the trained astronaut would be able to detect a steady light approximately equal to an 8th magnitude star.

For the observer in the orbiting CM/SM who must visually acquire the LEM's beacon against the earthlit lunar surface, the problem is more restrictive. As computed earlier, the background illumination of the moon from the "half earth," (B_{F_m}), is 1.77×10^{-5} candle-cm $^{-2}$. Then the background brightness at the eye is:

$$B_{F_a} = 0.25 \left(\frac{1.27}{2.1} \right)^2 (1.77 \times 10^{-5}) = 1.62 \times 10^{-6} \text{ candle-cm}^{-2}.$$

From Fig. 3, $E_a = 2.0 \times 10^{-12}$ lumen-cm $^{-2}$.

The threshold of illumination incident on the lens is then:

$$E_a = \frac{2 \times 10^{-12}}{0.25} \left(\frac{0.7}{1.27} \right)^2 = 2.43 \times 10^{-12} \text{ lumen-cm}^{-2}$$

C. REQUIREMENTS FOR SHORT-DURATION FLASHES

The problem of detecting flashing lights is complicated by the additional variable, time. "The sensation of luminosity takes a finite time to build up, reaching a maximum after an interval of which the magnitude depends on the amount of light in the stimulus. It is obvious that as the length of the flash increases it must eventually become equivalent to a fixed light. It is likely, though not axiomatic, that the effect of a very brief flash on the eye will be proportional only to the product of the illuminance and the time."⁴

Many renowned physiologists and physicists have investigated the effects of short-duration light stimuli, but the classical paper is that of Blondel and Rey in 1911, who noted that the nearer the illuminance to the threshold of the human eye, the longer it took to discover it.⁵ They formulated an empirical equation which approximated the plot of experimentally derived data for flashes of durations from 0.1 to 1.0 sec.:

$$\frac{E_{Fa}}{E_t} = 1 + \frac{0.21}{t}$$

Toulmin-Smith and Green (1933) later surmised that different results would be obtained for different supra-luminal values.⁶ By alternately viewing a steady light of known conspicuity (illuminance E_c at the eye) and a flashing light of period t , they adjusted the intensity of the latter until the two seemed equally conspicuous. From the results of many tests, they derived a more applicable empirical equation:

$$\frac{E_a}{E_f} = \frac{kt}{a+t}$$

where k and a are both functions of the parameter E_c .

Their formula was modified by Hampton in 1934 to the form that is now used in most cases to determine the threshold illumination for a blinking light.⁷

$$\frac{E_a}{E_f} = \frac{t}{\left[\left(\frac{0.0098}{E_c}\right)^{0.81} + t\right]}$$

where E_c is measured in lumen-km⁻².

In Section B, we showed that the threshold illumination, (E_a), that must be apparent at the eye when looking at the star field background is 1.0×10^{-13} lumen-cm⁻². The illumination of a third magnitude star incident on the objective lens is 1.55×10^{-11} lumen-cm⁻² in the absence of any atmospheric absorption. At the eye this would be changed by the telescope formula to:

$$E_c = 0.25 \left(\frac{1.27}{0.70} \right)^2 (1.55 \times 10^{-11}) = 1.28 \times 10^{-11} \text{ lumen-cm}^{-2}$$

Or $E_c = 0.128 \text{ lumen-km}^{-2}$

Now the illumination of the flash apparent at the eye can be found as a function of the duration of the flash:

$$\frac{E_{fa}}{E_f} = \frac{\left[\left(\frac{0.0098}{E_c} \right)^{0.81} + t \right]}{t} = \frac{1.0 \times 10^{-13}}{t} (0.125 + t) \text{ lumen-cm}^{-2}$$

For small values of t (between 1 and 100 microseconds) the t in the numerator can be neglected.

Then:

$$E_{fa} = \frac{1.25 \times 10^{-14}}{t} \text{ lumen-cm}^{-2}$$

A plot of required apparent illumination versus effective flash duration is shown on Fig. 4. For a flash whose effective duration is 10 microseconds, the required illumination is 1.25×10^{-9} lumen-cm $^{-2}$ at the eye. Again using the telescope formula, the required illumination on the objective lens is found to be:

$$E_{fr} = \frac{1.25 \times 10^{-9}}{0.25} \left(\frac{0.7}{1.27} \right)^2 = 1.52 \times 10^{-9} \text{ lumen-cm}^{-2}$$

or $E_{fr} = 1.41 \times 10^{-6} \text{ lumen-ft}^{-2}$

At the maximum distance of 450 nautical miles this illumination requires an output intensity at the source of $(1.41 \times 10^{-6}) (450 \times 6080)^2 = 10.6$ million beam candlepower.

The intensity of a flashing beacon to be observed as conspicuous as a third magnitude star against the moon must also be computed. In Section B, the threshold of illumination (E_a) was computed as 2.0×10^{-12} lumen-cm $^{-2}$ at the eye viewing the lunar surface that is brightened by "half earth" light.

Thus:

$$E_{fa} = \frac{2.0 \times 10^{10} \left[\left(\frac{0.0098}{0.128} \right)^{0.81} + t \right]}{t} = \frac{(2.0 \times 10^{-12})(0.125)}{t}$$

$$E_{fa} = \frac{2.50 \times 10^{-13}}{t} \text{ lumen-cm}^{-2} \text{ or } 2.32 \times 10^{-10} \text{ lumen-ft}^{-2}$$

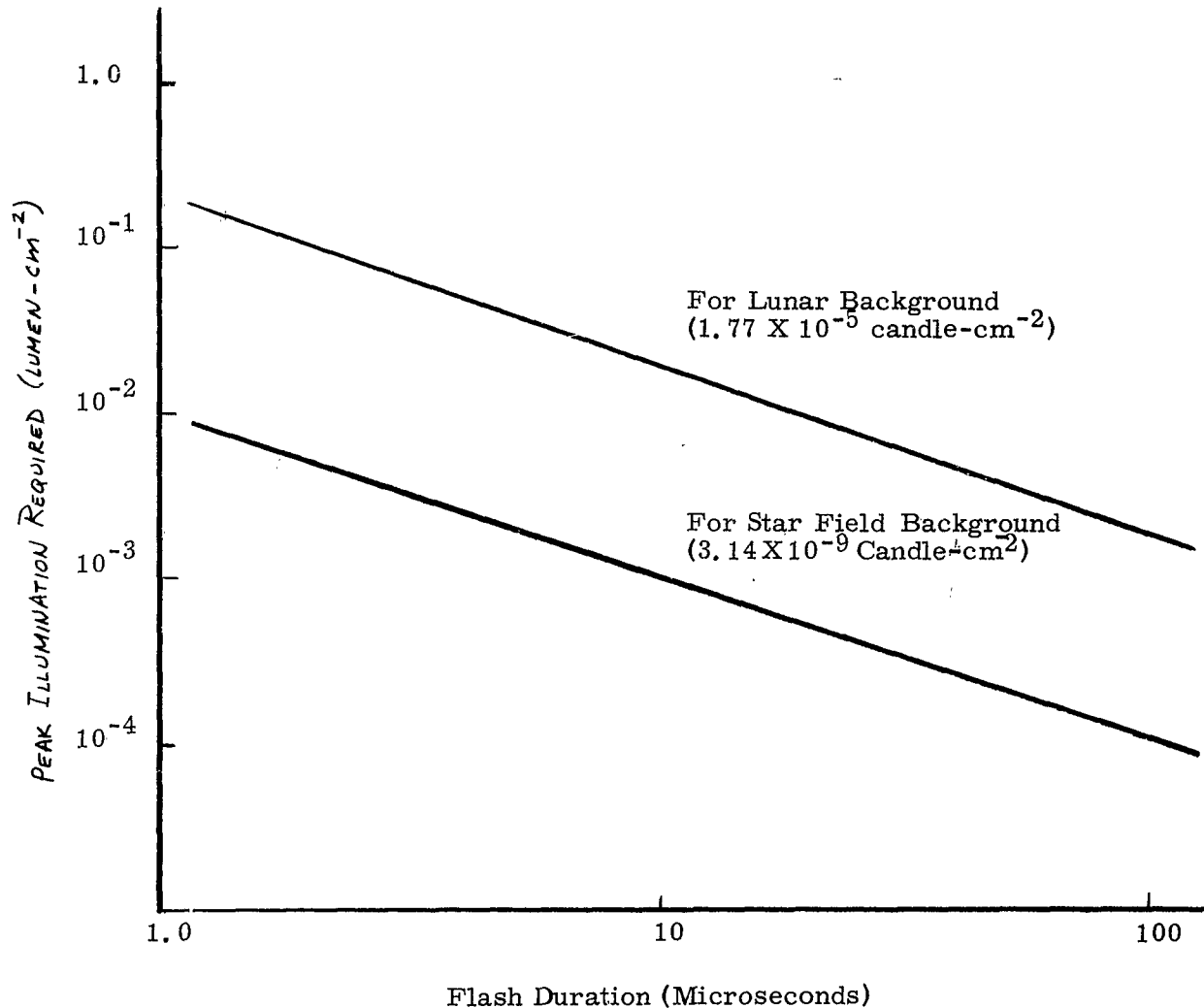


Fig. 4. Parameters of a 3rd Magnitude Star Equivalent Flashing Beacon

This is also plotted on Fig. 4. For a 10 microsecond flash the peak illumination required at the eye is 2.32×10^{-5} lumen-ft $^{-2}$. The illumination on the objective lens must be:

$$E_r = \frac{2.32 \times 10^{-5}}{0.25} \cdot \frac{0.7}{1.27}^2 = 2.80 \times 10^{-5}$$
 lumen-ft $^{-2}$

At the maximum distance of 450 nautical miles, this requires an output intensity at the source of $(2.80 \times 10^{-5})(4.50 \times 6080)^2 = 210$ million beam candlepower.

Since a maximum source intensity of 210 million beam candlepower in each 10 microsecond flash is needed for the LEM's beacon, this means it must supply at least 2100 beam candlepower seconds energy every time it is triggered.

Containing the beam in a reflector with a gain of 10 permits a reduction of the output energy requirement to:

$$CPS = \frac{2100}{10} = 210 \text{ candlepower-seconds/flash}$$

For a nominal efficiency of 4 candlepower/watt or $4 \frac{\text{CPS}}{\text{Joule}}$ then this requires an energy/flash of

$$\text{Energy/Flash} = 210/4 = 52.5 \text{ Joules/Flash}$$

Recent vacuum tests simulating space environment by the firm of Edgerton, Germeshausen and Grier have shown that their commercially available xenon flashlamps continued to operate without noticeable deterioration in performance at an average power of 100 watts with only radiation cooling. A nominal repetition rate of one flash per second at 52.5 Joules/flash is therefore well within the capability of the flashlamp.

If this same energy level were maintained as the CM/SM ap-

proached the LEM until the source appeared as conspicuous as a first magnitude star, the distance to the source would be 179 miles (See Fig. 5). Then if the apparent intensity were maintained at that level as the range was further reduced, the energy/flash could be decreased (See Fig. 6).

Two major obstacles to precise ranging are jitter in the flash-lamp circuitry and relatively slow rise times for the light pulses. Jitter may be defined as the random variation in the inherent time delays from the time of receipt of the initial flash at the CM until the subsequent flash begins. Uncertainty in time measurements due to jitter and rise time limitations lead directly to errors in range. For a nominal accuracy of 1% in range from 445 nautical miles to 2 NM, one can ascertain the accuracies in time measurements which are necessary. For example, at 2 NM, a 1% accuracy will only allow an error given by:

$$\text{Error} = \frac{(.01)(2)(1.15)(1.609 \times 10^3)}{3 \times 10^8} = 0.12 \text{ microseconds}$$

A linear relationship exists for the various ranges, and the result is contained in Fig. 7.

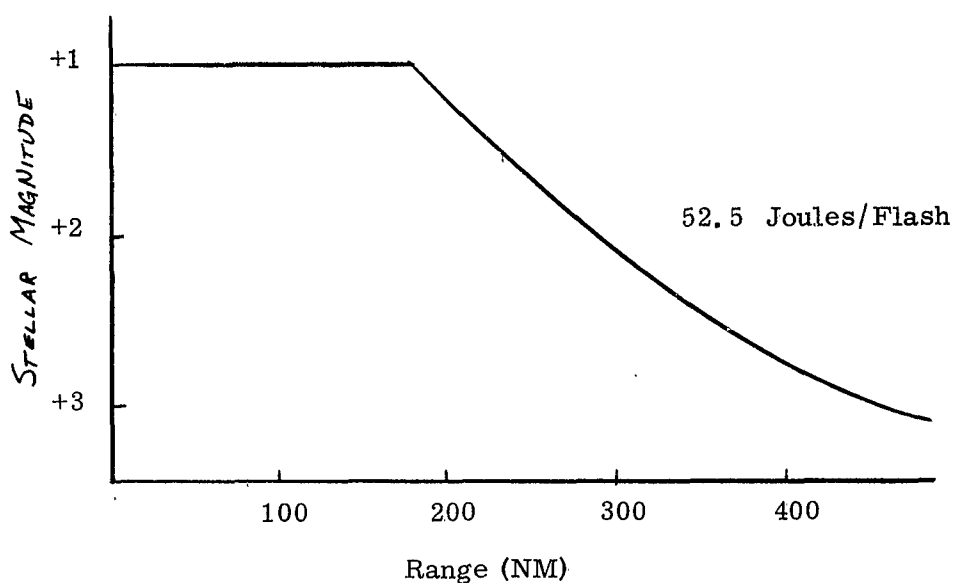


Fig. 5. Stellar Magnitude Versus Range
for Constant Energy

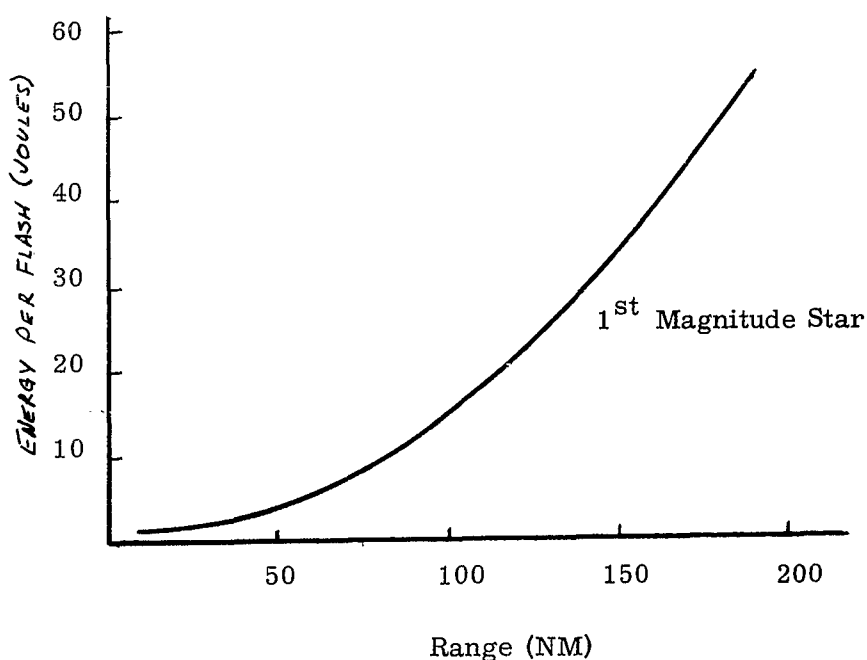


Fig. 6. Energy Per Flash Versus Range
for Constant Stellar Magnitude

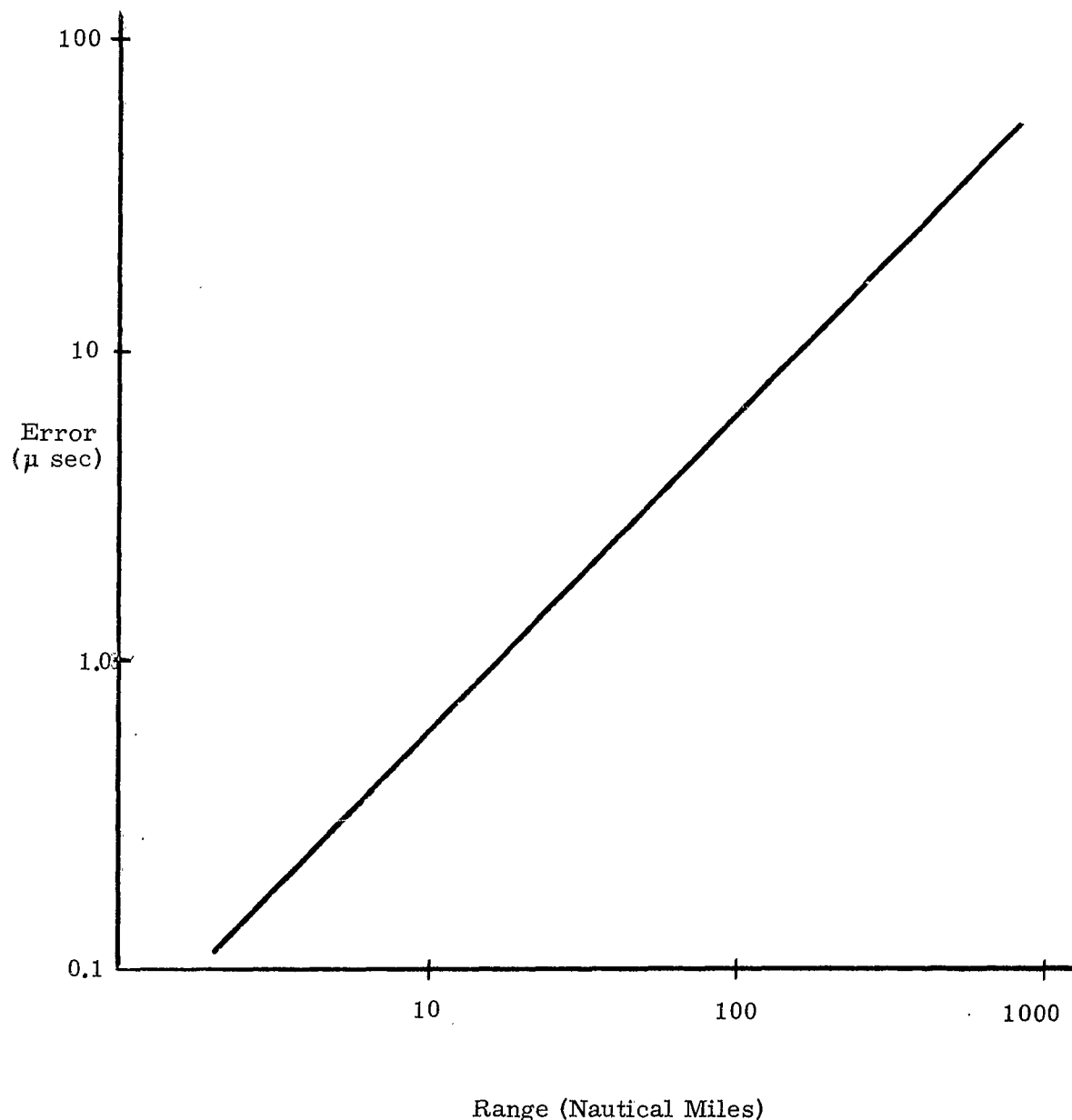


Fig. 7. Allowable Error Versus Range
for 1% Accuracy in Range

D. SYSTEM COMPONENTS

The variation of light output intensity with time for xenon flash-lamps follows very closely the variation of current with time.⁸ The maximum current and thus the maximum output light intensity is a function of the energy. The rate of change of the current, or the rise time of the light pulse, is independent of the tube voltage, depending instead chiefly on the characteristics of the energy storage capacitor and the dynamic resistance of the flash tube.

During very rapid discharge, a capacitor exhibits the characteristics of a tuned circuit; that is, the current oscillates with a particular frequency which is a function of the capacitance and the inductance inherent in the capacitor. In particular, the current will oscillate at a frequency given by $f_0 = \frac{1}{2\pi\sqrt{LC}}$ when the resistance in the circuit is very small. This frequency is commonly referred to as the "ringing frequency." The rise time of the light pulse will never exceed 1/4 of the period of this frequency. For rapid rise times it is therefore necessary to have high ringing frequencies, which in turn requires small values of capacitance and inductance.

DC-DC converter weight considerations limited the maximum supply voltage to 20,000 volts. For a nominal repetition rate of one flash per second the maximum energy per flash is limited to 100 Joules (from the 100 watts maximum average power consideration). The energy in a charged capacitor is given by $W = \frac{CV^2}{2}$. If one assumes that all the energy is discharged through the flashlamp, then the largest capacitance which could be considered is 0.5 microfarads. The combination of the above factors led us to select a range of capacitances

from 0.01 to 0.5 microfarads for preliminary experimentation.

In the conventional use of flashlamps, where the voltage does not exceed 4,000 volts, the entire voltage is applied across the terminals of the flashlamp and an external triggering pulse is applied to flash the tube.⁹ Since the 20KV that we selected was considerably above the self-flash voltage of the tube, it became necessary to hold off this voltage until the flash was desired by some device such as a spark gap or thyratron. Because of the large currents that flow when the tube is fired, we decided to use a spark gap rather than a thyratron as the hold-off device.

Two different xenon flashlamps presently manufactured by the firm of Edgerton, Germeshausen and Grier were selected for testing. The FX-38A flash tube, which is nominally rated at 100 Joules per flash with a three inch electrode spacing and a dynamic arc resistance during discharge of 1.0 ohm, was selected for preliminary testing of the triggering circuitry. The FX-42 flash tube with the same length arc but a nominal rating of 600 Joules per flash and a dynamic resistance of only 0.3 ohm was used for rise time measurements. Rise time is directly related to the time constant (approximately RC) of the discharge capacitance and flash tube resistance.

Several different light sensitive devices were considered. A photomultiplier appeared to be the only device capable of exhibiting the sensitivity needed at the longer ranges. For shorter ranges and for laboratory testing, we utilized vacuum phototubes and solar cells. Work is being done concurrently to perfect a circuit sensitive to small changes in light intensity but utilizing solar cells which have the advantage over photomultipliers in that they are relatively insensitive

to steady background illumination.¹⁰

At first, it was suspected that the noise level in the photomultiplier circuit might obliterate the pulses received from the flashlamp. The sources of this noise are:

- (1) Dark current
- (2) Noise-in-signal
- (3) Variations in the background

Dark current is that residual current present when the cathode is not illuminated. It is caused by the thermionic emmission of the photocathode, ionization of residual gas, ohmic leakage, light feedback, and charging of the glass envelope. It amounts to 0.04 microamps for the IP21 when operating at design voltage.

The noise-in-signal is present only when a signal is present. It is caused by the statistical nature of the photoelectric emission for a fixed level of incident illumination. The average tube current is constant but the instantaneous current fluctuates around the average with an RMS value given by:

$$i_n = \sqrt{2eI\Delta f}$$

where $e = 1.6 \times 10^{-19}$ coulombs

I is the average photoelectric current in amperes
 Δf is the bandwidth of the system (including the amplifiers and photomultiplier) in cycles per second.

For this system the bandwidth requirement is approximately 5 megacycles in order to observe a rise time of 0.2 microseconds.

We have shown that the field brightness of the lunar surface observed without an optical aid is 1.77×10^{-5} candles-cm⁻². The

illumination that this brightness produces on the objective lens is 1.69×10^{-6} lumen-cm $^{-2}$ (See Appendix A). Upon transmission through the telescope the illumination would be concentrated into a circular spot of 1 cm diameter on the photocathode. There the illumination found by the telescope formula would be 6.82×10^{-7} lumens-cm $^{-2}$. Therefore, the average number of lumens striking the cathode would be 5.35×10^{-8} lumens. The 1P21 has a sensitivity of 80 amps per lumen which yields a DC tube current (I) of 42.7 microamps. This exceeds the recommended maximum tube current of 10 microamps, but one could use a 0.7 neutral density filter in the system to reduce the illumination received to one-fifth its initial value. Then the D. C. tube current would be 8.55 microamps. The noise-in-signal produced by this D. C. background level would be 3.7×10^{-3} microamps. This is negligible compared to the dark current. Since the dark current and the noise-in-signal are statistically independent, the RMS of the total effect approximates that of the dark current alone.

The peak amplitude of the desired signal illumination on the objective lens was shown to be 3.0×10^{-8} lumen-cm $^{-2}$. At the photocathode this would be 1.22×10^{-8} lumen-cm $^{-2}$. The peak number of lumens falling on the cathode would be 9.55×10^{-9} lumens but the 0.7 density filter reduces this to 1.91×10^{-9} lumens. The signal current would then be 0.153 microamps. Therefore the signal to noise ratio of this circuit would be 3.85 to 1. This is adequate for detection.

Finally, several optical components were assembled or modified to simulate the 3X viewing telescope to be used on the space vehicles. Only the illuminations from the field of view transmitted through the optical system were projected onto the photo-emissive surface of a photomultiplier.

CHAPTER II

EXPERIMENTAL PROCEDURES

A. HIGH VOLTAGE

The selection of high voltages dictated that certain precautions be observed when operating the associated equipment. DANGER - HIGH VOLTAGE signs were conspicuously placed on the door and wall to conform to the Building Code specifications. A sturdy grounding cable was rigged and the equipment was properly grounded. As a further precaution it was decided that the high voltage equipment would not be operated unless at least two persons were physically present in the room. Care was taken to insure that all leads were properly insulated and whenever possible the high voltage terminals were situated so as to be difficult to be inadvertently touched during operation of the equipment.

A high voltage power supply was purchased (See Fig. 8) which had a safety relay that cut off the supply when current in excess of 5 ma was present. The supply was initially connected directly to the energy storage capacitor which resulted in the actuation of the relay each time the capacitor was discharged. This safety feature was eventually by-passed after excessive use of the relay resulted in its failure. The relay was replaced and thereafter a charging resistor was used in series with the power supply to limit the current.

The flashlamp was initially placed in series with the spark gap

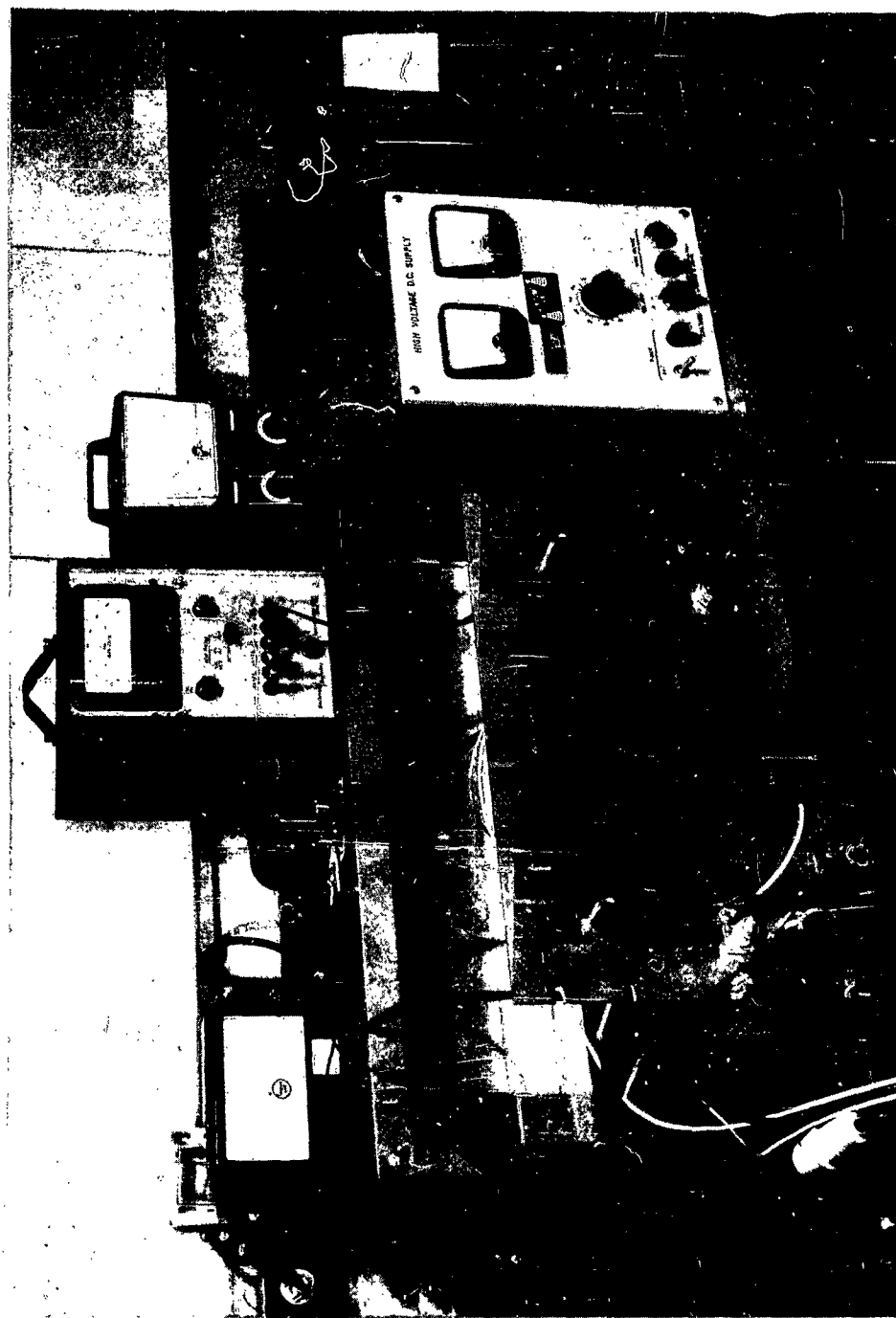


Fig. 8. Power Supplies, Trigger Circuit, and Transponder

but between the high voltage terminal of the energy storage capacitor and one side of the spark gap. This was done in order to operate the spark gap with one electrode at ground potential and to eliminate the necessity of isolating the trigger electrode (See SPARK GAPS, CHAPTER III). In this configuration, with the flashlamp "floating" at the high voltage, corona effects were sufficient to cause the xenon to partially ionize. When a resistor was placed in parallel with the flashlamp in an attempt to stabilize the circuit, the ionization was still present. This undesirable effect, coupled with the fact that reflector mountings would have to be completely insulated, led to the interchange of the flashlamp and spark gap.

Corona effects were also present in other parts of the circuitry. It was necessary to file down all sharp points and in some cases to apply a liquid insulation (which dried upon contact with air) to persistent sources of corona.

B. SPARK GAPS

Having selected a spark gap in air as the hold-off device, we had one built to our specifications.¹¹ This gap has adjustable electrode spacing through the use of a micrometer head. We purchased two pairs of ball bearings which were then hollowed to fit over the electrode extensions (6 mm stainless steel). One pair is naval brass and these have a 3/4" diameter. The other two are nickel-copper-bronze with a 1" diameter. The trigger electrode is 2 mm stainless steel wire. The electrode extensions and the trigger electrode are mounted on a single piece of bakelite 1 cm. thick.

We initially triggered the gap by applying a 30KV spike to the trigger electrode, which arced to the lower potential ball. The resulting ionization of the air was adequate to break down the gap and the main discharge occurred. There were several disadvantages with this method: (1) the trigger probe in the high potential field required an isolation transformer to avoid damaging the trigger circuit; (2) exact control of the main discharge depended on the amount and spatial distribution of gaseous ions in the gap which varied greatly from flash to flash. In many attempts these conditions were insufficient to trigger the main discharge.

A similar problem in controlling a high voltage plasma discharge in a shock tube was recently solved by Arthur Lewis of the MIT Electrical Engineering Department. We decided to assemble a similar triggering arrangement. This consists of biasing the trigger electrode midway between the potential of the two discharge electrodes such that the trigger electrode does not materially affect the electrical field

between the discharge electrodes. Triggering is then accomplished by bringing the trigger electrode to ground potential, and with proper spacing of the electrodes, the gap breaks down and the main discharge occurs. The method of bringing the trigger electrode to ground potential is explained in detail in the next section.

The first spark gap was dangerous to use for two reasons: (1) it was open on all sides, and (2) less than 1 cm. of bakelite separated the 20KV electrode from the bench. Therefore, we designed and fabricated a new spark gap which also included two biasing resistors for the trigger electrode and a specified resistance to terminate the transmission cable (See TRIGGERING CIRCUIT). We selected 1/2 inch bakelite and utilized nylon screws throughout. The spark gap was accessible on only one side, and the high voltage terminals were recessed to avoid accidental contact during use. We threaded a 3/16 inch stainless steel rod for the trigger electrode and two 1/4 inch stainless steel rods for the electrode terminals. This configuration gave us trouble when flashing at high flash rates, and we found that by removing the "top" of the enclosure and ventilating the air gap with a fan the trouble was eliminated. (See Fig. 9) Apparently, ozone or nitrous oxide generated during the discharges inhibited successive discharges of the gap.

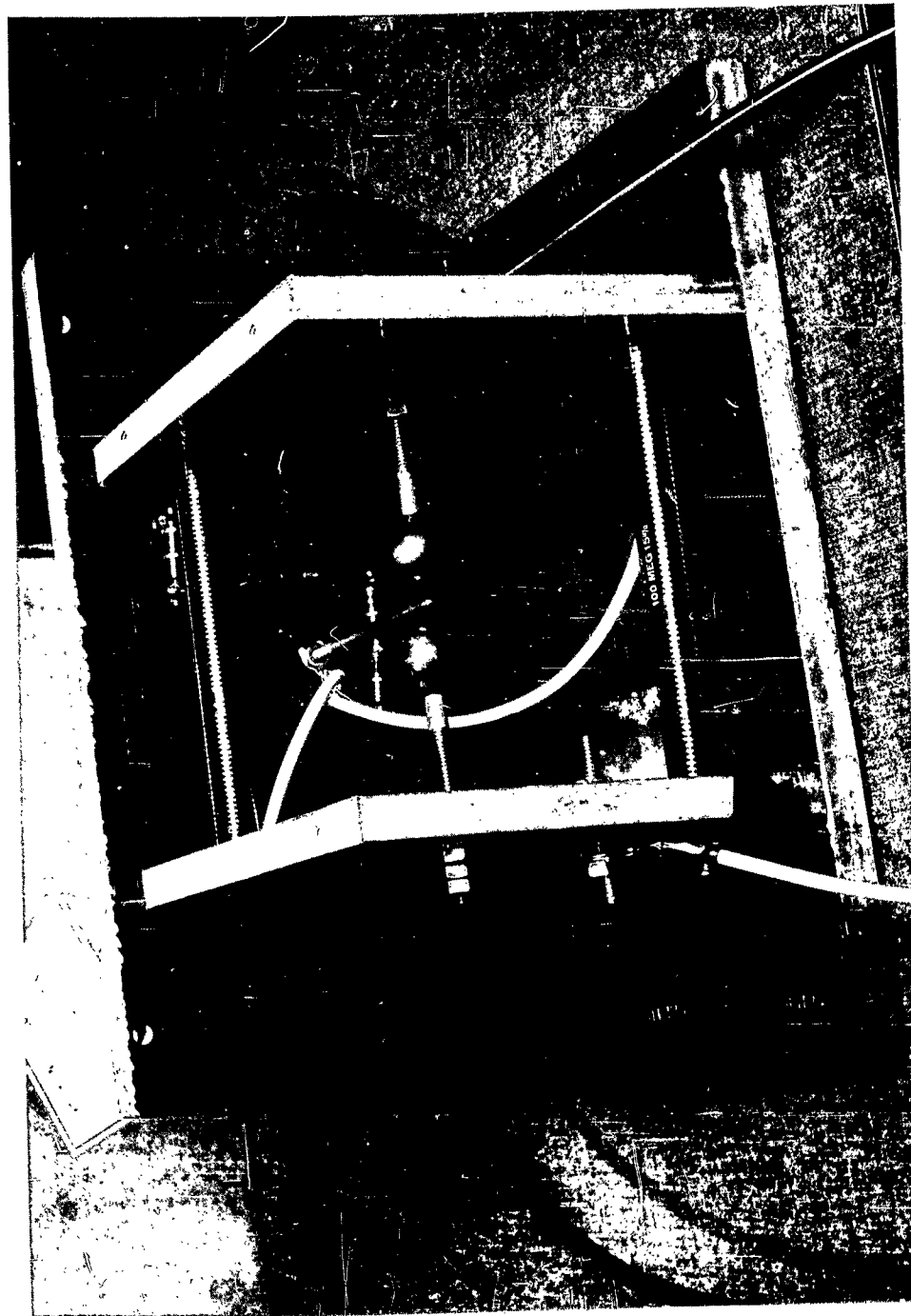


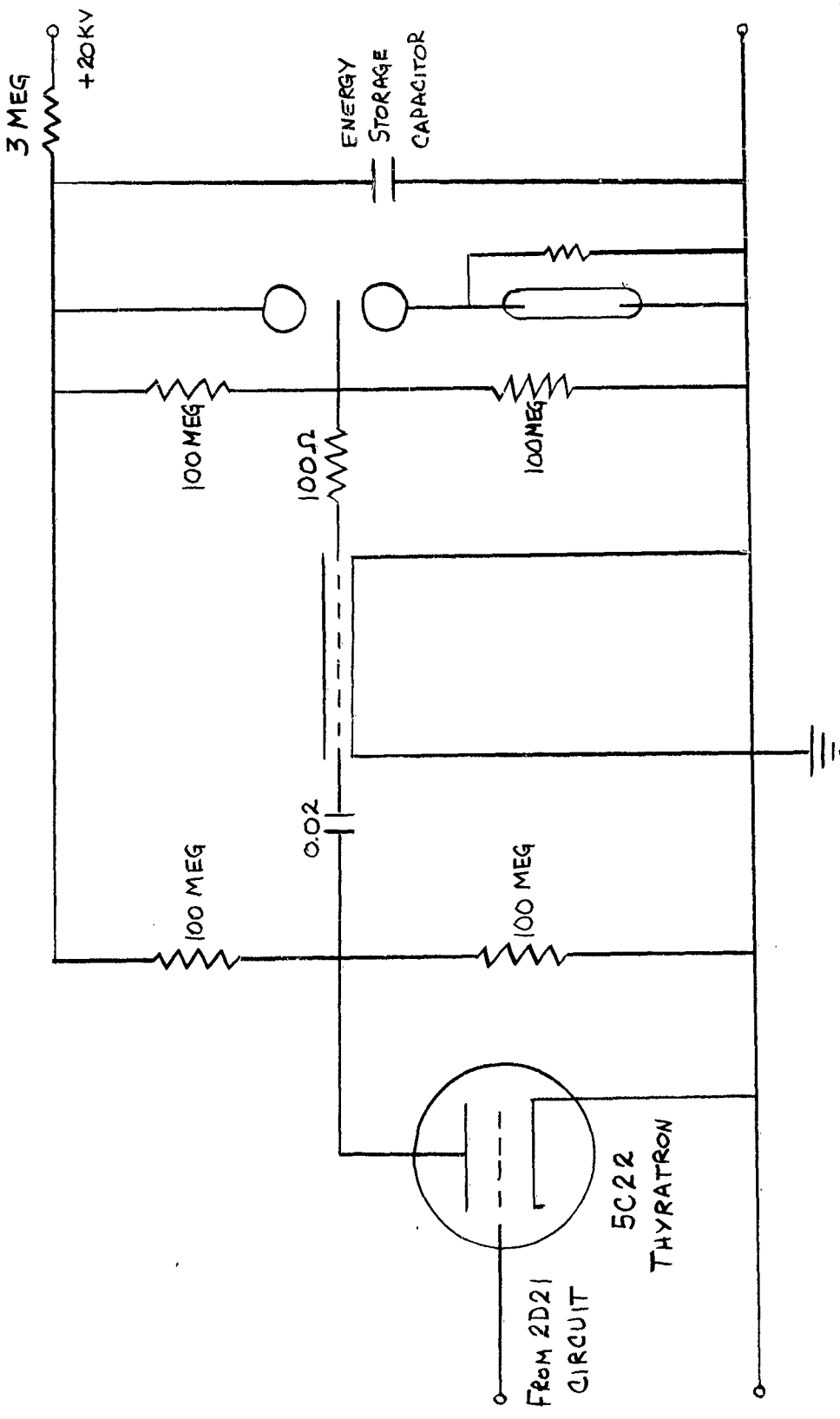
Fig. 9. Close-up of Spark Gap

C. TRIGGER CIRCUIT

The trigger circuit we fabricated utilizes a 5C22 hydrogen thyratron to bring the trigger electrode of the spark gap to ground potential upon command from either a manual switch or a signal from the transponder. The plate of the 5C22 is biased at half the voltage applied to the terminals of the spark gap, and is thus at the same potential as the trigger electrode. The two are physically connected by means of fifteen feet of RG-62U transmission cable, which is terminated at the thyratron with a capacitor and at the trigger electrode with a 100 ohm resistor. When the thyratron is fired, the plate of the 5C22 and the trigger electrode are brought to ground potential, which fires the spark gap. The 100 ohms resistance approximately matches the impedance of the transmission cable to prevent pulse reflections. The capacitor limits the energy through the 5C22 during discharge. (See Fig. 10)

The 5C22 is fired by a 2D21 xenon thyratron which supplies a negative pulse of 400 volts with a rise time of 20 nanoseconds. The circuit diagram for this circuit is shown in Fig. 11. The trigger circuits plus the associated rectifiers, transformers, and a cooling fan are mounted on a 13" X 17" X 4" chassis with a standard 10" relay rack panel on the front so that it may be rack mounted in an aircraft for airborne testing. (See Figs. 8 & 12)

FIG. 10. TERMINATION OF TRIGGER CIRCUIT WITH SPARK GAP AND FLASHLUE



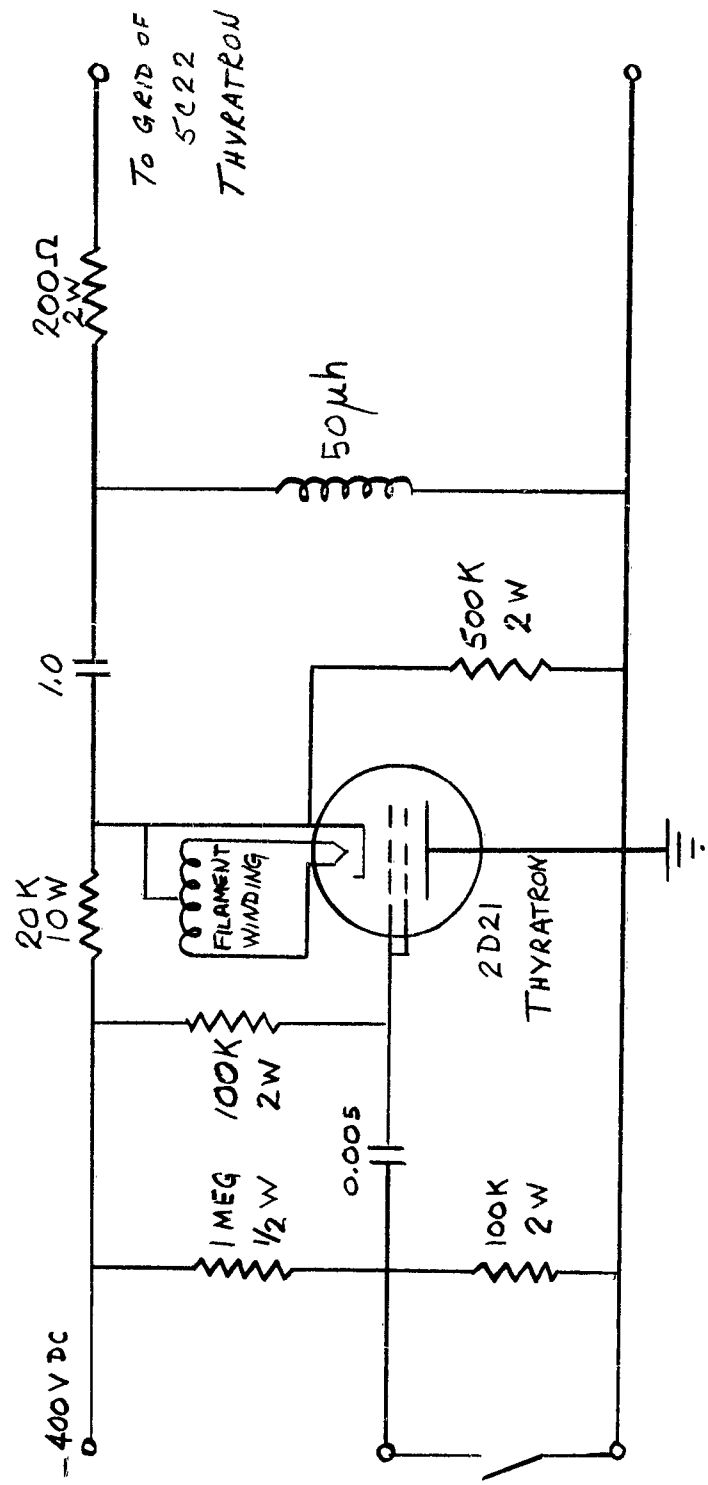


FIG. 11. FIRST STAGE OF TRIGGER CIRCUIT

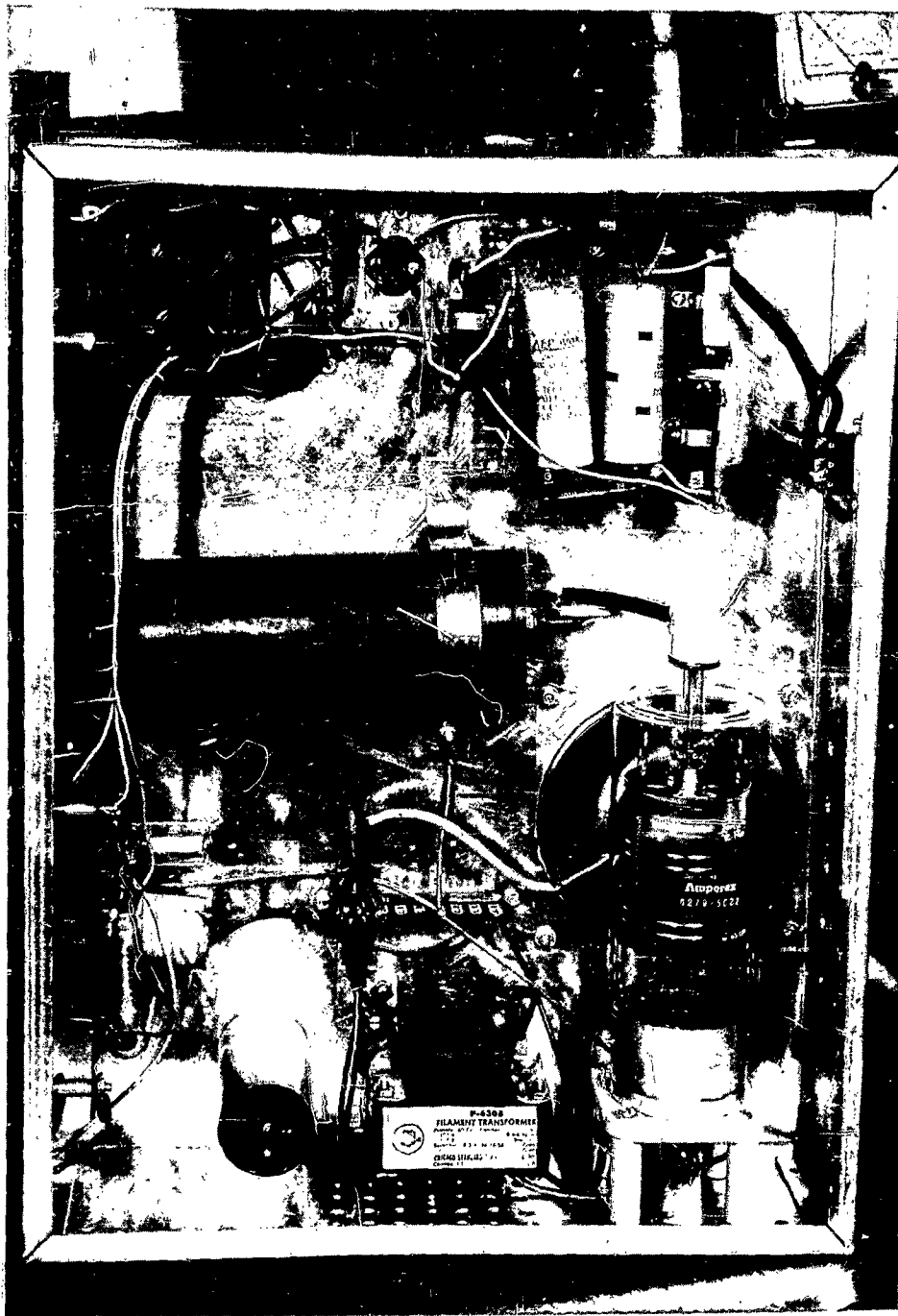


Fig. 12. Close-up of Trigger Circuit

D. PHOTOSENSITIVE DEVICES

Fast and accurate displays of all of the different light output waveforms produced by the various combinations of voltages and energy storage capacitors was one of the earliest design and fabrication steps accomplished. Many photosensitive pickup devices were available for consideration. A versatile pickup device which was borrowed from the laboratory of Professor Edgerton allowed a choice of four different sensitivity settings to cover a wide range of illuminations.¹² However, at faster time constant settings it was only useful for observing low intensity sources. The photo tube was often over saturated in spite of the use of neutral density optical filters and peak intensities could not be properly measured.

Consequently, a simple photo tube circuit composed of an RCA #929 photoelectric tube and a single-stage amplifier was built and its circuit diagram is shown below:

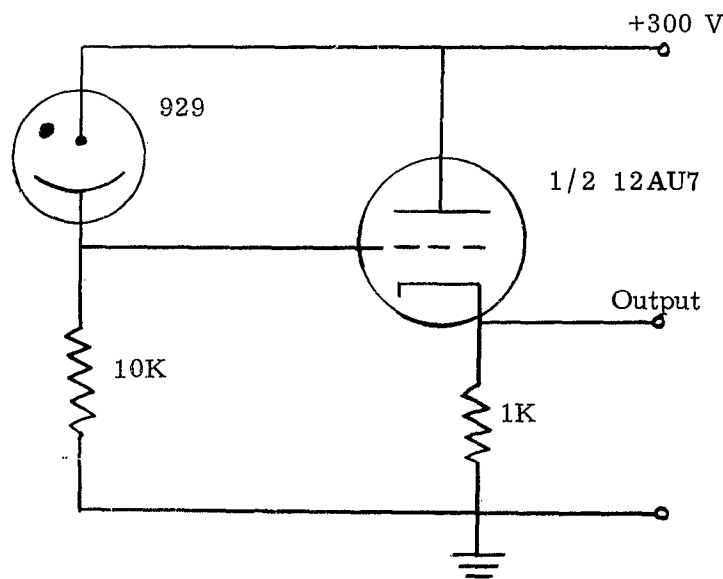


Fig. 13. Transponder

The standard used to calibrate this pickup device was a special xenon flash tube #L5908-2 obtained from Professor Edgerton's Strobe Laboratory at Massachusetts Institute of Technology. It displays a well-defined output of 7434 lumens-seconds per flash and reaches a peak luminosity of 276.9 lumens. The peak horizontal candlepower is rated at 2.48 million. When the #929 phototube circuit, powered by 300 V DC from a Beckman/Berkeley Regulated Power Supply, Model 702A, was placed 10 feet from the lamp, its output signal displayed on an oscilloscope reached a peak of 60.0 volts. This was the average of three readings. The ratio of illumination received versus voltage output was $0.449 \text{ lumens-cm}^{-2}$ per volt. This pickup device then became the standard for all photometric measurements in this experimental thesis. Output readings as large as 80 volts were recorded without any apparent waveform distortion due to saturation of the photocathode.

For long-range detection, where the signals received would be of very low intensity, the pickup device described above would be inadequate. A photomultiplier tube circuit (Fig. 14) was constructed with an RCA 931-A photomultiplier for use with a 3X telescope that would be capable of detecting short duration light pulses. This combination will be referred to as Assembly #1. The photomultiplier's photocathode was placed at a distance from the ocular such that the image of the field of view had diverged to a size only slightly smaller than the dimensions of the photocathode's S-4 surface. Thus concentration of the light into a spot from a fixed steady source such as stars in the field of view was avoided. For ranging measurements that were conducted in the daylight, a long range expedient was evolved using an

elbow 8X telescope with an 8° cone angle for its field of view. The photosensitive device used was an RCA 1P21 photomultiplier tube. This combination will be referred to as Assembly #2.

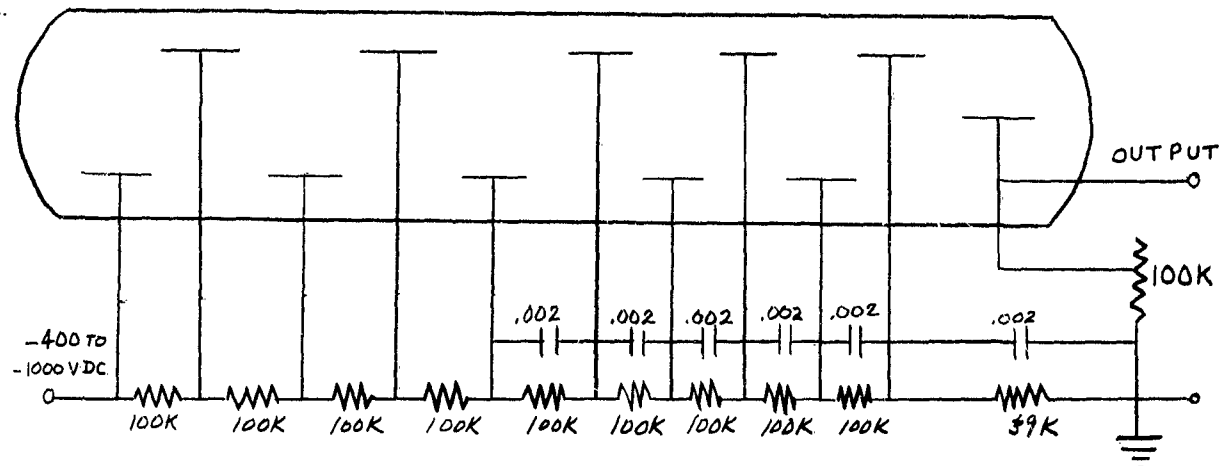


Fig. 14. Photomultiplier Circuit for Use with 931-A or 1P21

E. REFLECTOR

A parabolically-shaped aluminum lamp shade was found that could be modified to support either the FX38A or FX-42 flash tubes along its central axis. The axial distance of the tube could be varied in order to permit some adjustment of the size of the beam. Ideally, if the source had been a point source, placing it at the focal point of the parabola would have resulted in a narrow, highly directional beam. A specially designed flashlamp shaped in the form of a helix to give a small source area would have been much better. Such a tube together with its own parabolic reflector was produced by Edgerton, Germeshausen and Grier for use in night aerial reconnaissance. This combination of lamp and reflector was produced under special contract and was called the LS-23A.

CHAPTER III

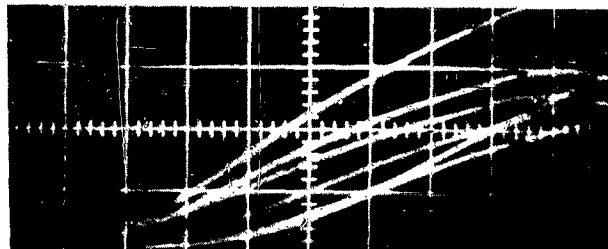
EXPERIMENTAL RESULTS

A. INTENSITY AND RISE TIME MEASUREMENTS

During the first week in the laboratory, a familiarization of the conventional use of xenon flash tubes was completed utilizing available equipment. The existing set-up included a 4KV laser stimulator power supply, a bank of capacitors totaling 380 micro-farads coupled through a 70 microhenry choke to an FX-42 flashlamp, and a special trigger circuit which supplied a 30 KV trigger pulse through a helix of wire around the flash tube. This configuration provided long, steady light pulses from the flashlamp.

The concept of placing a very short "impulse" of high voltage into the tube circuit to produce a "spike" of less than 0.1 micro-second duration on the output waveform was considered. Anticipating that any inductance in the tube circuit would delay the fast surge of current needed to produce this spike, we eliminated the choke from the circuit and selected a single, 25 microfarad, capacitor which was connected to the flashlamp terminals by short leads. It was noted that the presence of the triggering helix induced self-flashing at 3000 volts.

Output intensity waveforms detected by a phototube device were displayed on the oscilloscope, which was triggered by a loop of wire around the triggering lead. Six results were obtained at 2850 volts and are shown on the multiple exposure photograph in Fig. 15. Any attempt to create an output spike at a particular intensity level on the



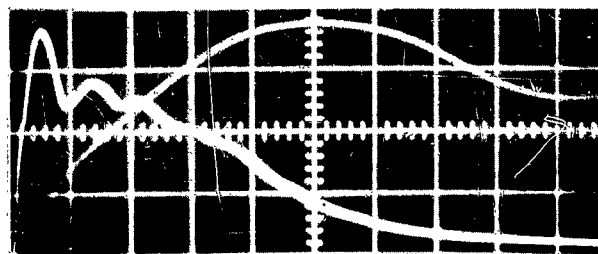
Sweep Rate: 1.0 usec/cm

Fig. 15. Early Jitter Detection

initial slope of those waveforms would obviously produce erroneous time measurements. Therefore, we chose to eliminate the impulse method altogether and adopt the simpler method of generating very fast rise times using voltages much higher than self-flash voltage and small energy storage capacitors. The problems in perfecting a proper hold-off and triggering circuit are discussed in a later section. The unnecessary triggering helix was removed.

A calibrated phototube was set up at a horizontal distance of 31.6 feet ($D^2 = 1000$) from the flashlamp and measurements were made of the output intensities, rise times and flash durations at voltages of 5, 10, 15 and 20 thousand volts using assorted capacitors. A parallel combination of the two largest capacitors was also used. A tabular list of the results is shown in Table 1.

Photographs of typical intensity waveforms are shown in Fig. 16. The double exposures were the result of recording two consecutive waveforms of the same energy flash at different sweep

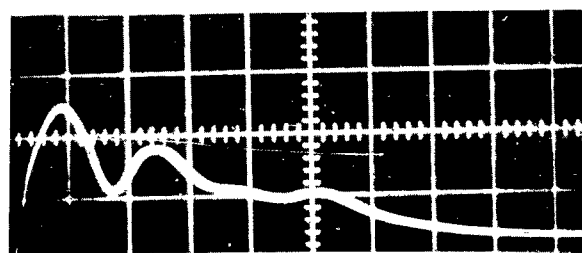


C = 0.5 μ f (energy = 100 Joules)

Slow sweep rate = 5 usec/cm

Fast sweep rate = .5 usec/cm

Period = 3.5 usec



C = 0.2 μ f (energy = 50 Joules)

Slow sweep rate = 2 usec/cm

Fast sweep rate = .5 usec/cm

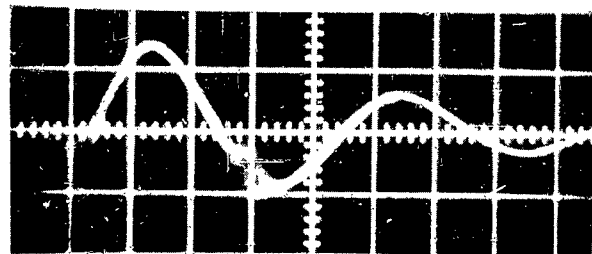
Period = 3.2 usec

Fig. 16. Intensity Waveform Photographs
at 20 KV with FX-42 Flashlamp

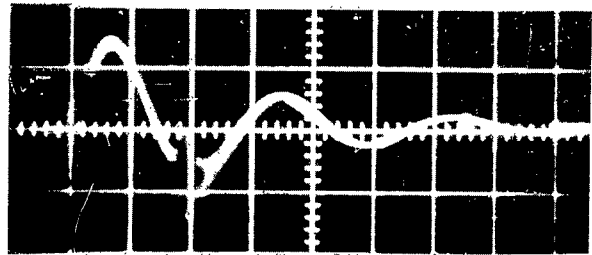
rates. Thus, we can accurately measure the rise time on the faster sweep rate exposure and at the same time observe almost the entire output waveform on the slower sweep rate exposure. The sinusoidal fluctuation, or ringing, was believed to be the result of capacitor ringing discussed in Chapter II. Pictures of the circuit currents were taken for verification. They were obtained by integrating the voltage induced in several turns of wire wrapped around the terminal lead to the lamp. Integration was performed by means of a simple RC circuit which had a time constant much larger than the period of the current oscillation. Fig. 17 shows the resulting current waveforms corresponding to the intensity waveforms shown in Fig. 16. The period of the current waveform is more than twice that of the intensity waveform when the 0.5 microfarad capacitor is used, and the ratio is not quite two when the 0.25 microfarad capacitor is used. If the current waveform is an accurate measure of the actual current in the lead to the lamp, then the conclusion is that the flash tube "rings" at higher frequency than the remainder of the circuit. This is certainly a questionable conclusion and a more sophisticated method of measuring current should be investigated.

The graphs of peak intensity versus capacitance and peak intensity versus voltage shown in Figs. 18 & 19 allow us to choose various combinations of capacitors and voltages to produce the same output peak intensities. In most instances it would appear advantageous to select the smallest capacitor in order to achieve the fastest rise time.

Fig. 20 shows that peak intensity versus input energy is relatively independent of capacitance. Fig. 21 shows that higher efficiencies are obtained at 15 KV than 20 KV, especially at lower



$C = 0.5 \text{ } \mu\text{f}$
Sweep rate = 2 usec/cm
Period = 8.2 usec



$C = 0.25 \text{ } \mu\text{f}$
Sweep rate = 2 usec/cm
Period = 5.4 usec

Fig. 17. Current Waveforms at 20KV
for FX-42 Circuit

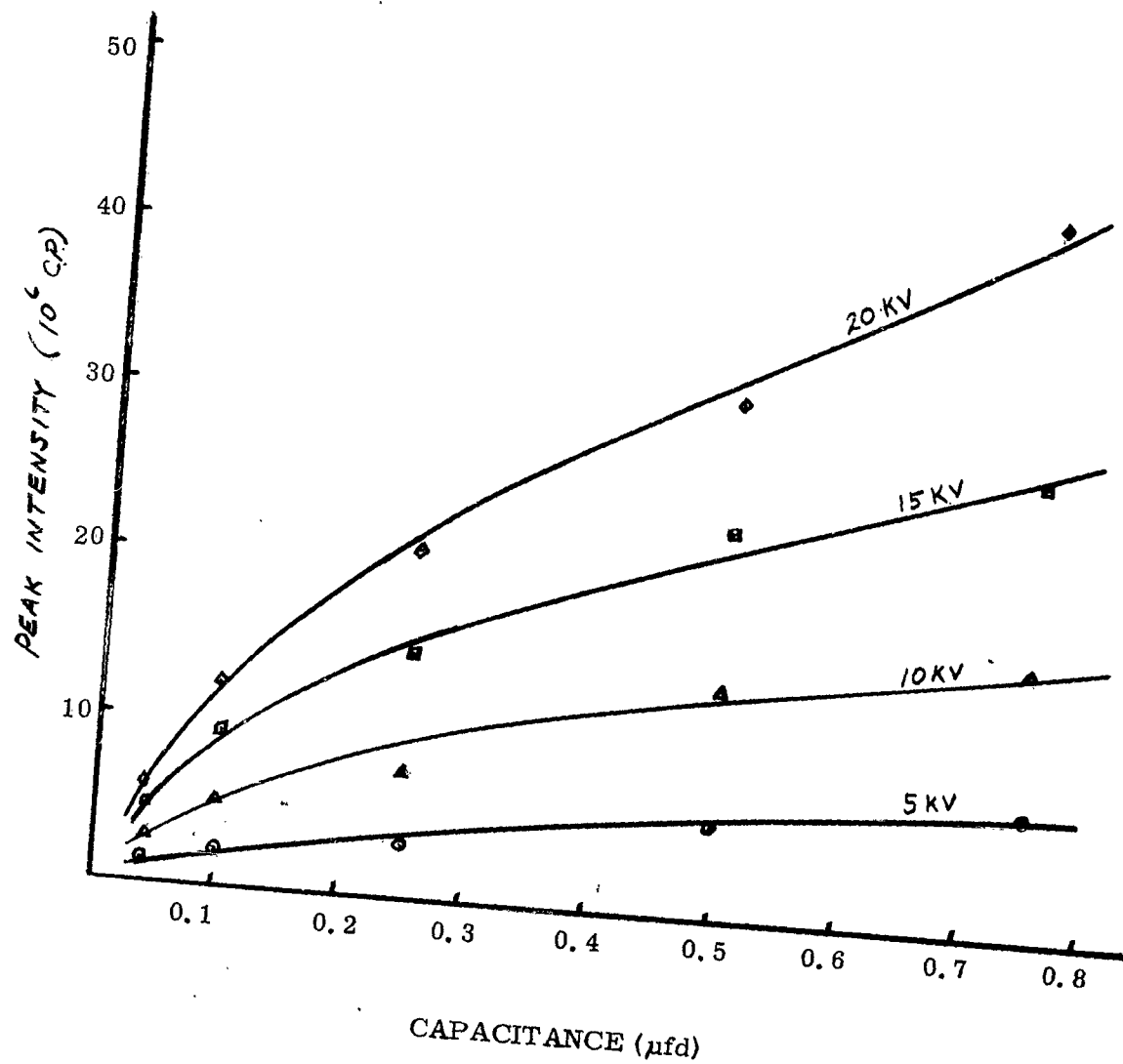


Fig. 18. Peak Intensity vs Capacitance for Different Voltages

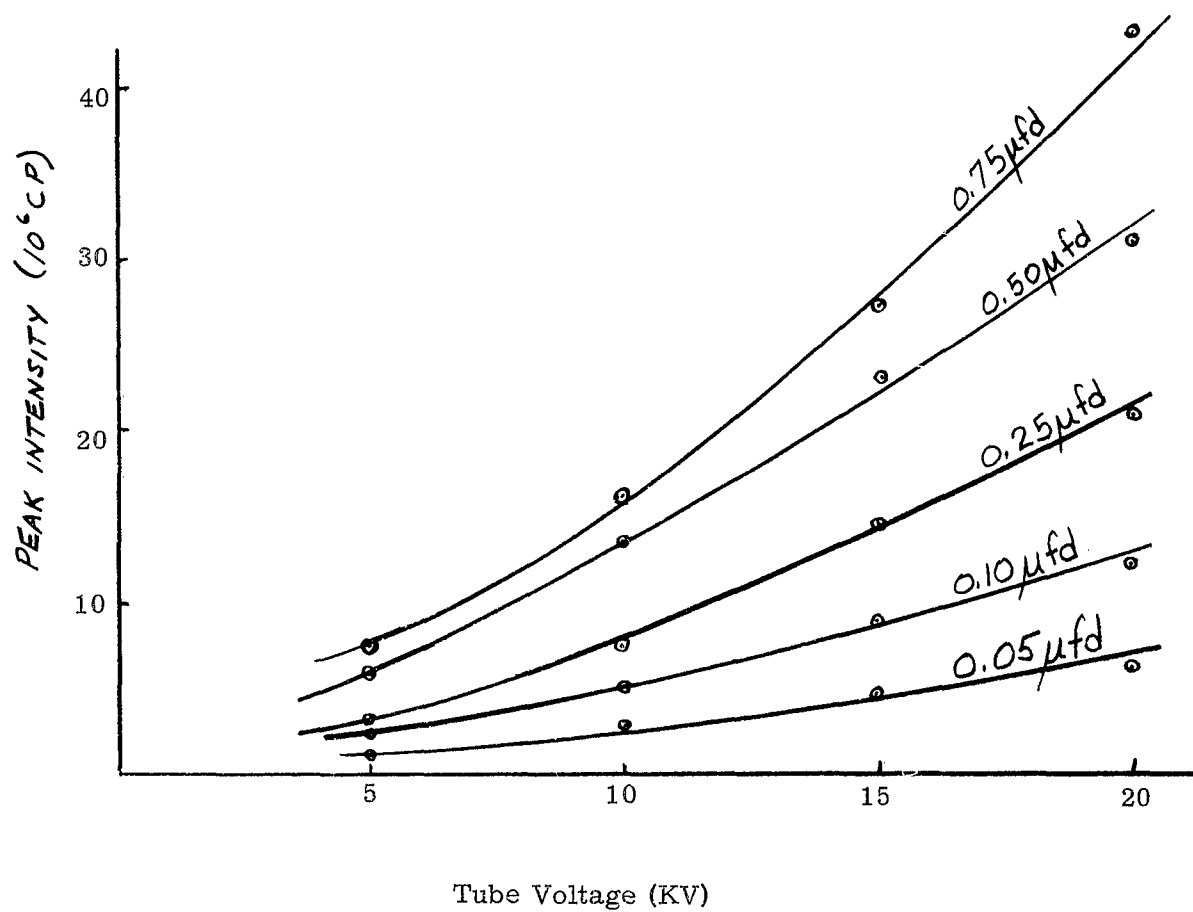


Fig. 19. Peak Intensity vs Tube Voltage for Different Capacitances

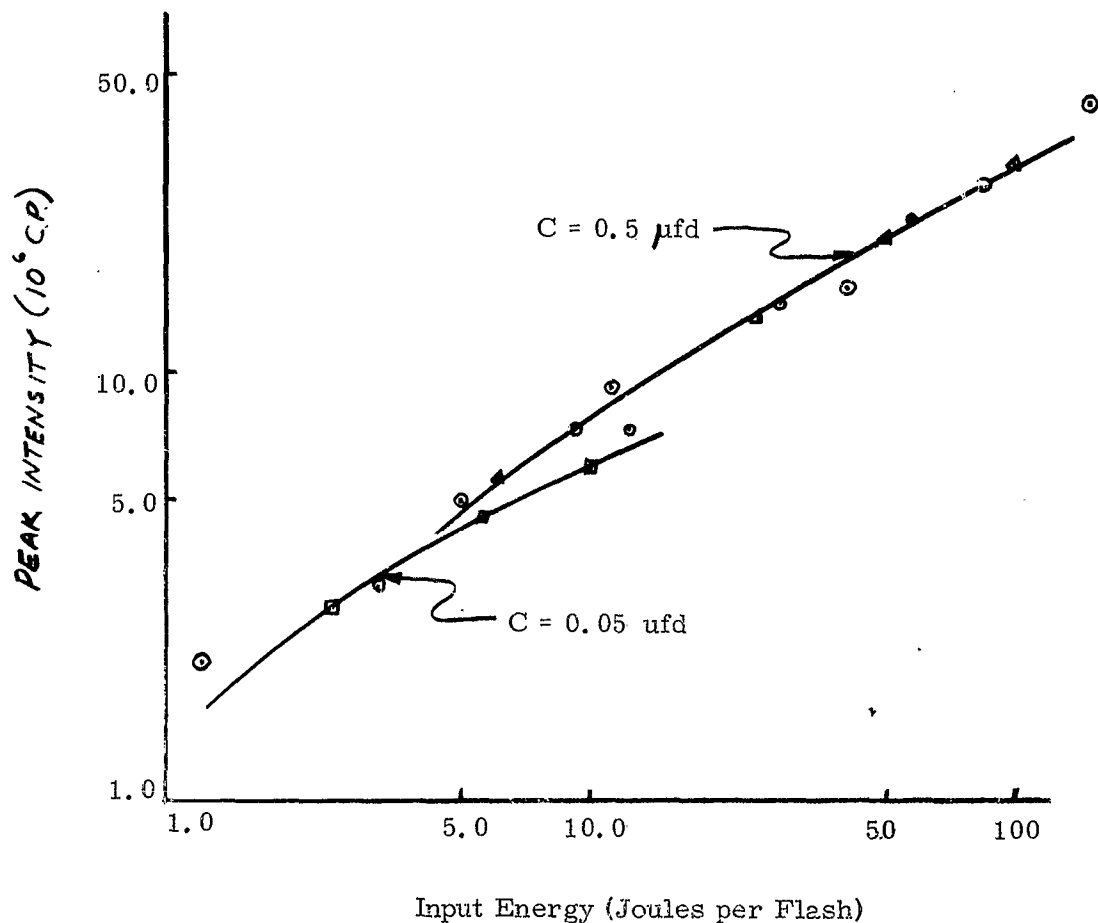


Fig. 20. Peak Intensity vs Input Energy for
Different Capacitances (Logarithmic Scale)

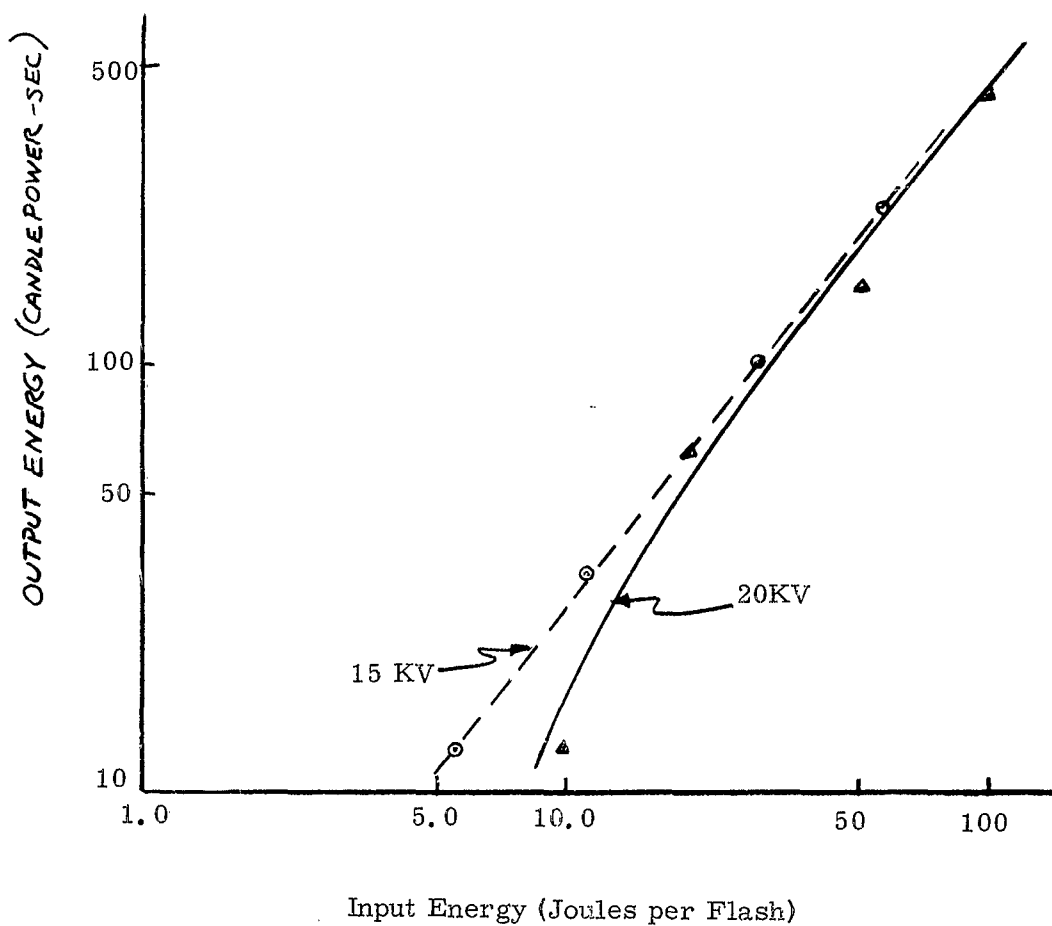


Fig. 21. Output Energy vs Input Energy for
Different Tube Voltages (Logarithmic Scale)

energies. For example, for 10 Joules input energy the 15 KV selection yields an output more than twice that for 20 KV (26.2 candlepower-seconds versus 12.5 cps). The energy measurements in candlepower-seconds in this figure were made by planimeter measurements of the areas enclosed by the output waveforms on individual photographs.

Graphs of rise time versus capacitance and rise time versus voltage show that rise times depend almost solely on the capacitance. (See Figs. 22 & 23). Less than 10% variance in the rise time is detectable over the ranges of voltages tested for each capacitor.

Analysis of the output waveforms shown in Fig. 16 reveals that high voltage operation of the flashlamp produces pronounced afterglow. The dissipation of the output waveform from peak intensity to less than one-third of that value takes many times the initial rise time. As a result, that decay interval is not as good an estimate of the flash duration as in the case of smaller voltages. Continued glow of the xenon at intensity levels below that which produces threshold visibility is essentially wasted.

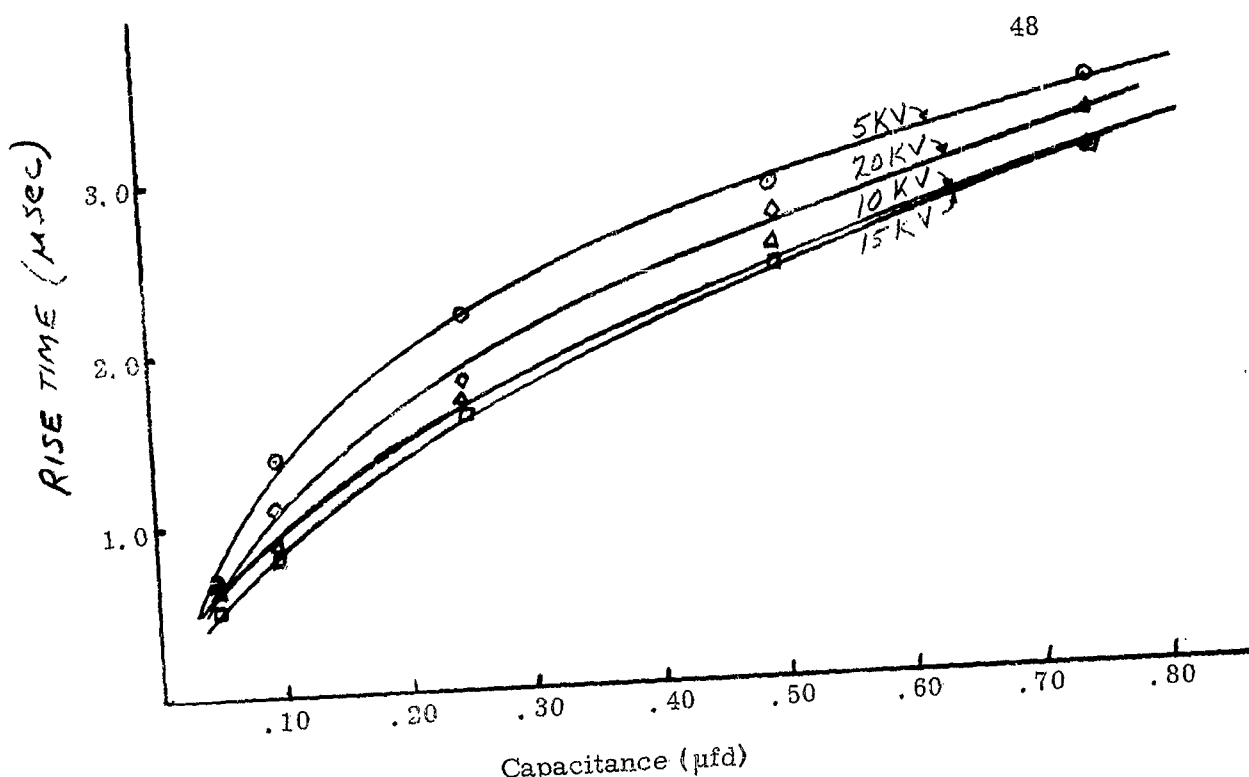


Fig. 22. Rise Time vs Capacitance for Different Tube Voltages

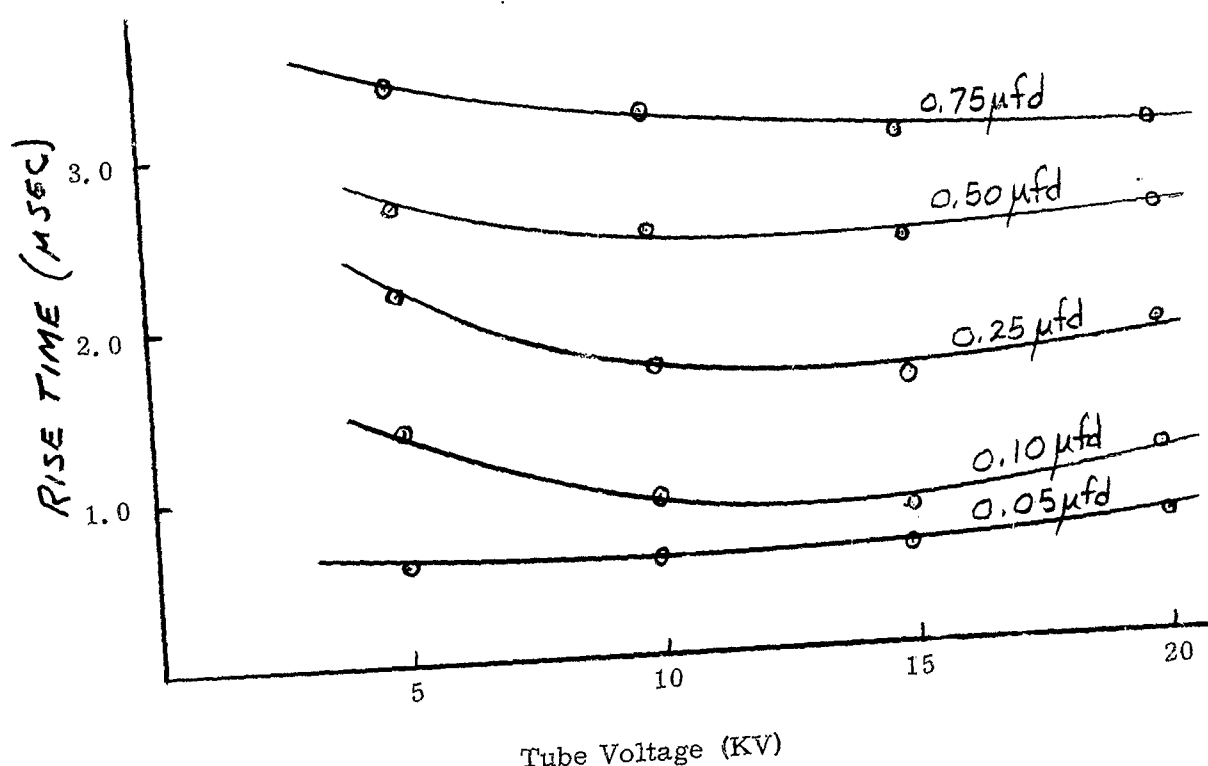
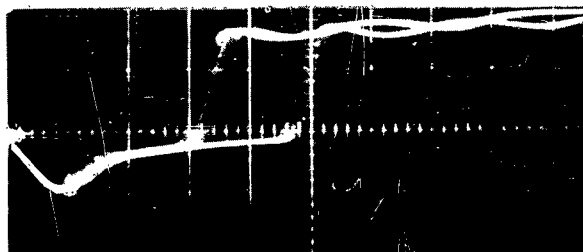


Fig. 23. Rise Time vs Tube Voltage for Different Capacitances

B. JITTER

Once the trigger circuit was completed, initial jitter measurements were made in the following manner: the transponder circuit supplied a pulse to the trigger circuit upon receipt of a flash from the Strobotac. Two Hoffman 55-C silicon solar cells were properly shunted so as to have output waveforms identical to that of the transponder. One of these solar cells received the same flash from the Strobotac as did the transponder, and the output of this cell was placed across one channel of the oscilloscope such that it triggered the sweep and displayed a negative-going pulse. The other solar cell received the subsequent flash of the FX-42 and its output was placed across the second channel of the oscilloscope as a positive going pulse. The two channels were added algebraically, and the result of three such flashes is shown in Fig. 24. The jitter was at least 3.4 μ sec.



Sweep Rate: 2 usec/cm

Fig. 24. First Jitter Measurement
at High Voltage

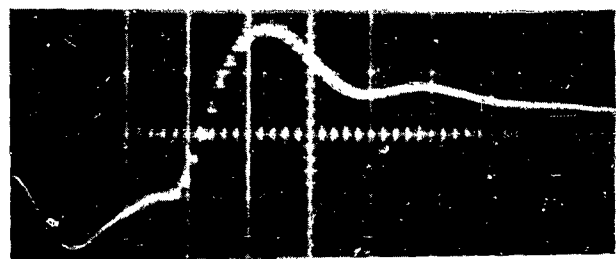
In order to pinpoint the jitter, we varied the technique slightly to sample the output of successive stages of the trigger circuit and displayed these signals on the second channel of the CRO. At sweep rates of 0.1 microseconds/cm. we were unable to observe jitter anywhere in the circuit up to the grid of the 5C22 thyratron. Removing the flashlamp from the circuit and observing the light from the spark gap alone revealed the continued presence of jitter. Therefore, the flashlamp was not the only possible source of jitter. Changing back to the open spark gap did not improve the results; the sources of jitter appeared to be concentrated between the grid of the 5C22 thyratron and the spark gap.

The resistor used to terminate the transmission cable consists of ten 2 watt, 10 ohm resistors connected in series (See Fig. 9) and they were carefully checked for loose connections, but none were found. The transmission cable was removed and carefully checked and found in satisfactory order. While the transmission cable was off, the trigger electrode of the open spark gap was connected to the capacitor by a simple lead and the system was tested. Pulse reflections were sufficient to cause arcing of the 5C22 and apparently destroy the tube.

Several 5C22 thyratrons manufactured in 1954 were secured from a local company. Although they had never been used, apparently sufficient hydrogen had leaked out to render them unfit for use. A new thyratron was ordered and during the interim period several changes were made in the circuit: (1) a small fan used to cool the 5C22 was disconnected, (2) the 0.02 μ f capacitor used to terminate the transmission cable at the trigger circuit was replaced by a 0.01 μ f capacitor (the original circuit called for this value but none were

readily available at the time), and (3) the 5C22 was placed in a vertical position on the advice of Professor Edgerton.

The results speak for themselves. Figs. 25 and 26 contain three sweeps each, as close examination will reveal. The jitter is evident in Fig. 26 and amounts to only 40 nanoseconds. At least a dozen sweeps were observed on photographs and the above results were consistently verified.



Sweep Rate = 0.5 usec/cm

Fig. 25. Later Jitter Measurements



Sweep Rate = 0.2 usec/cm

Fig. 26. Expanded View of Fig. 25.

C. REFLECTORS

By recording the illuminations received on a pickup device as it was moved halfway around the FX-42 from one end to the other at a constant distance in a plane which contained the longitudinal axis, we established a locus of points in that plane which received equal illumination from the lamp. If the curve connecting those points were rotated 360° around the longitudinal axis of the tube, the surface of the figure evolved would be the three-dimensional locus of points of uniform illumination. The total area of the surface which receives an illumination of 100,000 lumens per square foot was computed to be approximately 3490 square feet. This means that when the lamp reaches its peak brightness it is radiating 3.49×10^8 lumens if the input energy is 100 Joules. The data used to compute the locus of points of equal illumination is contained in Table II. A projection of the surface on the horizontal plane is shown in Fig. 27.

We attempted to concentrate as much of the luminosity pattern as possible into a conical beam which subtends a solid angle of $\pi/4$ steradians at the lamp. If the luminosity pattern were perfectly spherical, the maximum theoretical gain achieved with a perfect reflector would be 16. If the output light were uniformly distributed over a sphere, the illumination received would be:

$$E = \frac{3.49 \times 10^8}{4\pi \times 1000} = 2.78 \times 10^4 \text{ lumens-ft}^{-2}$$

The peak illumination received in the horizontal plane without any reflector was $3.10 \times 10^4 \text{ lumen-ft}^{-2}$. Therefore, the best theoretical gain possible for the FX-42 lamp whose output were uniformly channeled

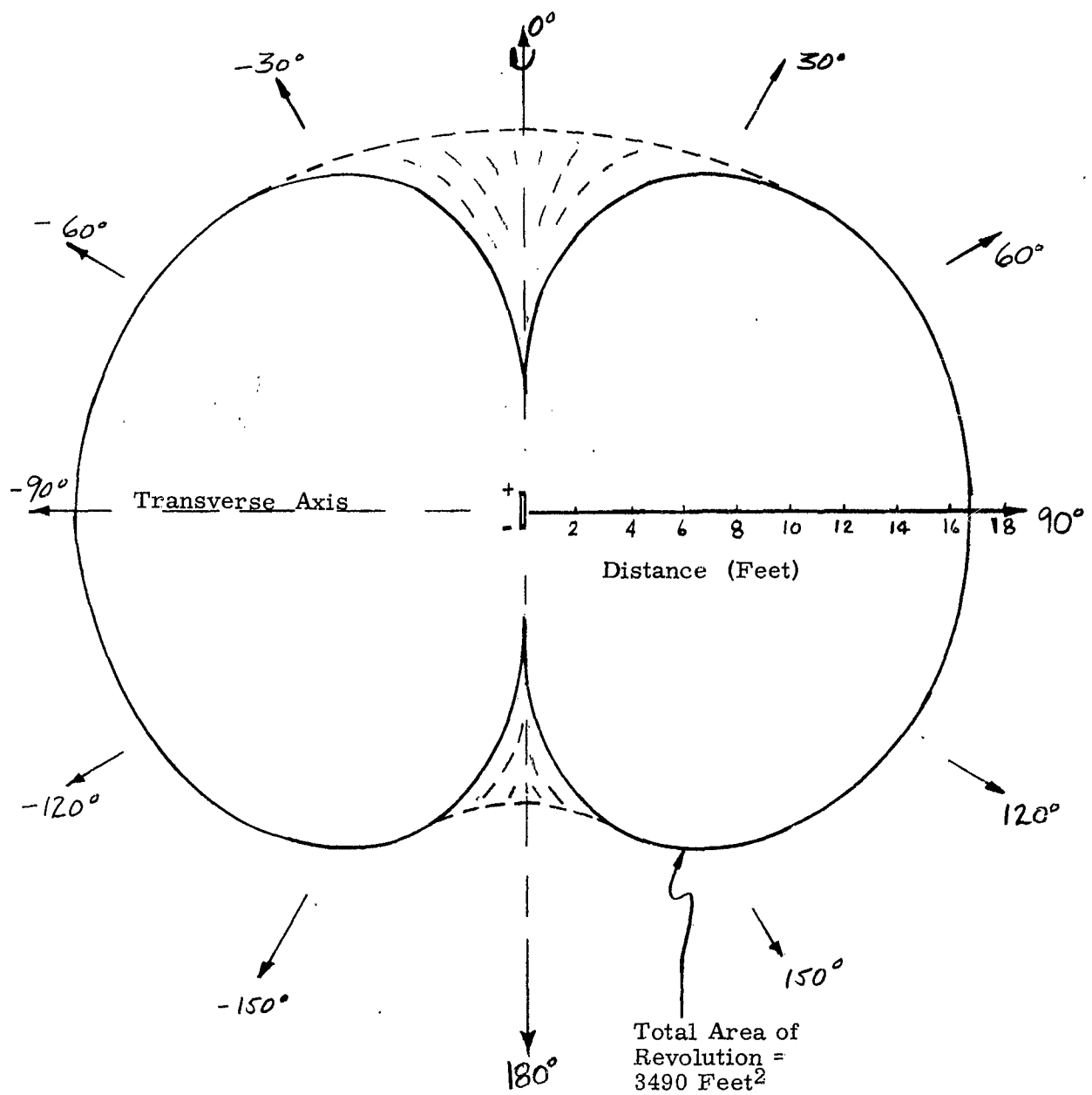


Fig. 27. Luminosity Pattern of FX-42 for an indicated uniform surface illumination of 100,000 lumens per Feet²

into the 57.8° circular cone would be:

$$G = \frac{2.78 \times 10^4 \times 16.0}{3.10 \times 10^4} = 14.35$$

Three different reflectors were tested. Type #1 (Fig. 28) was constructed from a six inch half-cylinder. The inner surface was covered with aluminum foil. The maximum gain in intensity recorded using this reflector was only 1.4. Also, it was obvious that the desired conical beam of $\pi/4$ steradian solid angle was not generated.

Type #2, (Fig. 29) consisted of a silver-coated concave mirror, which subtended a cone angle of 60°. The best intensity gain (2.9) was realized when the center portion of the arc was focussed by the mirror at the plane of the photocathode and this adaptation of the circular mirror is not practical for two reasons:

1. The beam is extremely narrow.
2. Only the small portion of the 3 inch arc located near the focal point has its output pattern contained in the beam.

The last reflector tested (Fig. 30) consists of a parabolic aluminum lamp shade. The orifice was machined to receive a 1.5 inch diameter cylindrical "slug" of nylon insulation 5 inches long which had been center-bored to carry the lead to the high voltage terminal of the flash tube. A clip fitted at the end of the nylon slug gripped the flash tube. The other end of the tube was supported in another clip mounted on a 2 inch ceramic standoff. This ceramic standoff was attached to the inside of the reflector 3 inches from the large end. This arrangement held the flash tube along the longitudinal axis of the reflector. A 10 ohm resistor was affixed to the outside of the reflector and connected in parallel with the flash tube to stabilize the spark gap. The inside

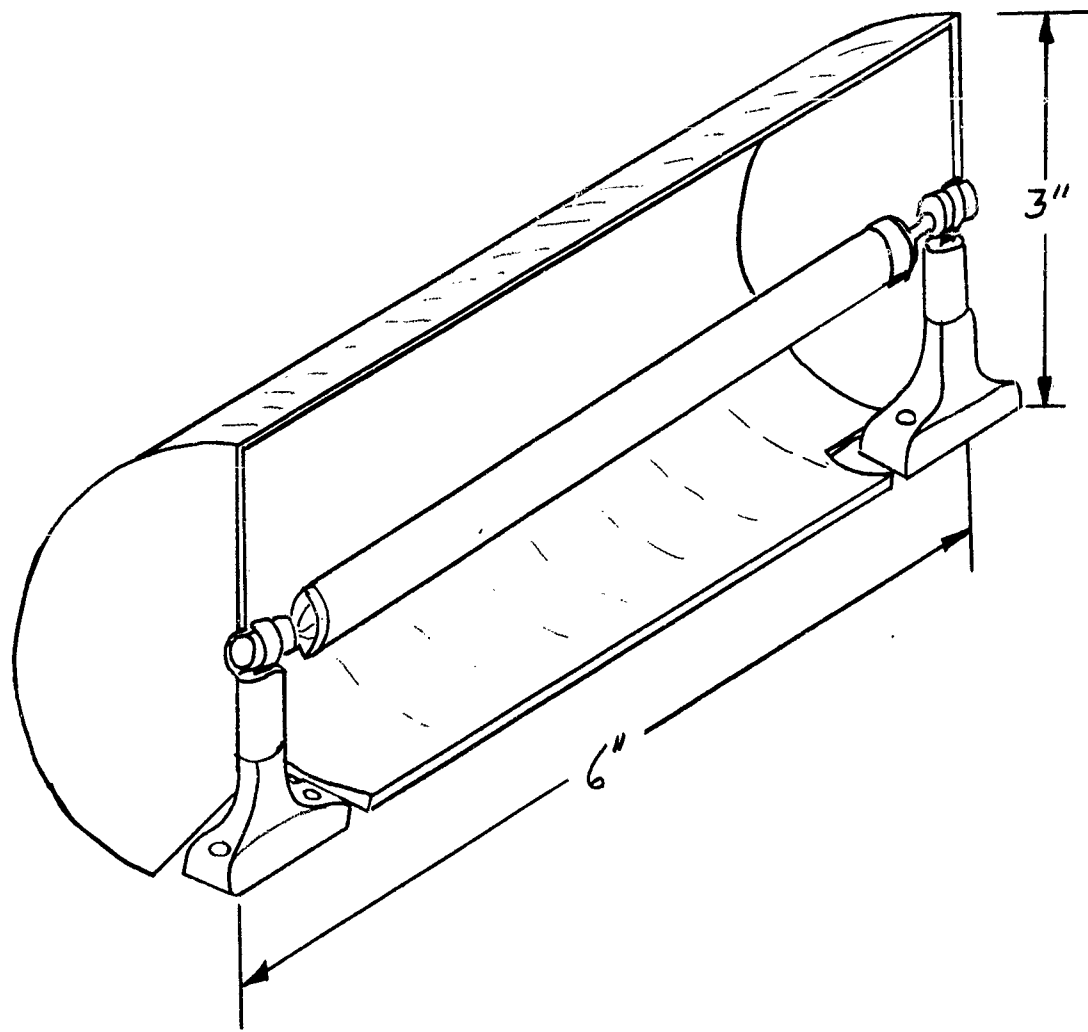


Fig. 28. Reflector Type #1

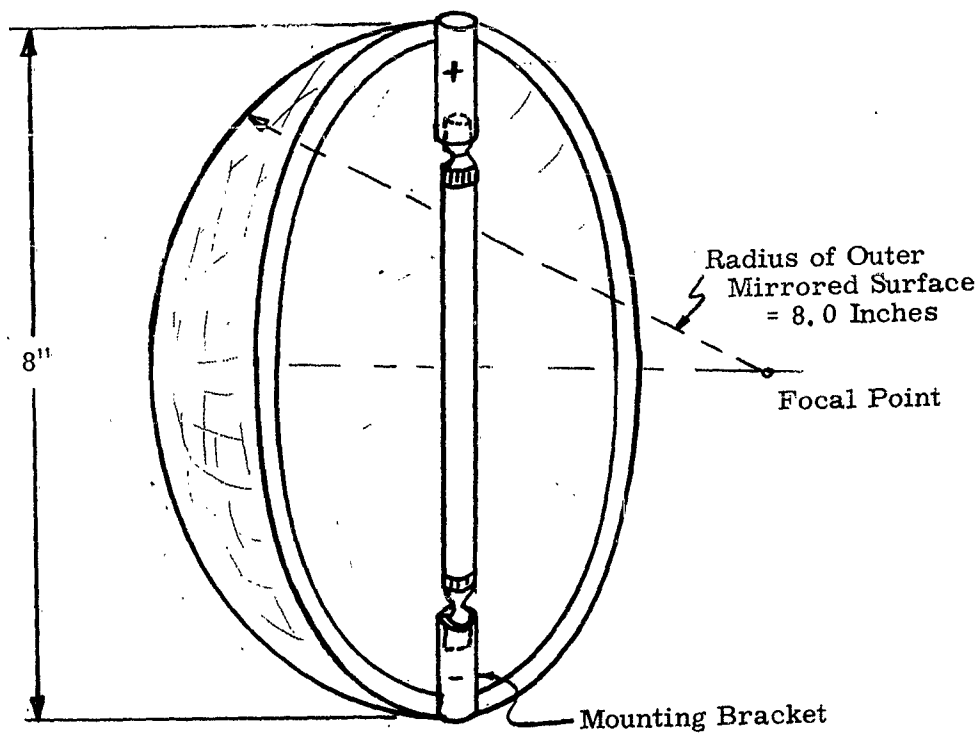


Fig. 29. Reflector Type #2

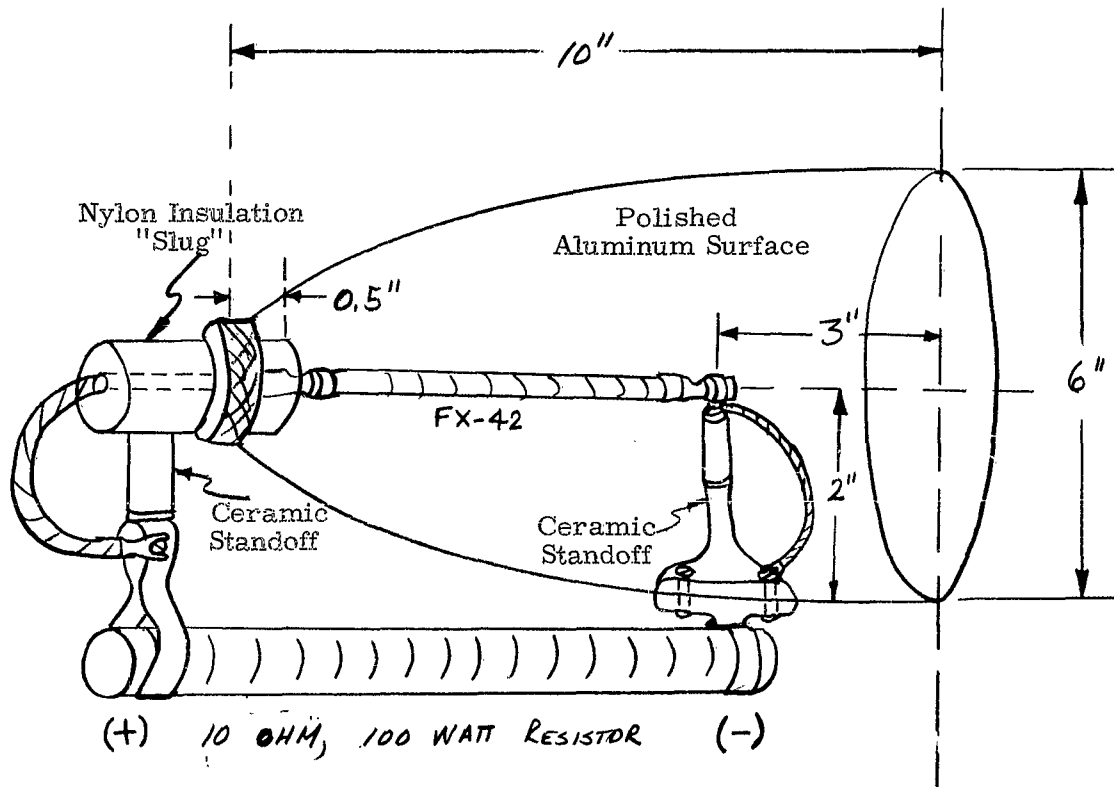


Fig. 30. Reflector Type #3

surface had been painted a dull black and was covered with aluminum foil to improve its reflectivity.

One measurement was made of the intensity produced along the central axis of the lamp at a distance of ten feet. The output voltage recorded from the phototube detector circuit was 6.0 times the peak voltage for the same flashlamp without the reflector. An attempt to improve the reflectivity of the inner surface was made by having it polished to a high luster.

The flashlamp and reflector were mounted on a telescope mount which permitted calibrated angle changes in the horizontal or vertical plane. Observations of the intensity were made at 7.5° intervals in the horizontal plane and 5.0° intervals in the vertical plane (See Table III). The vertical plane contained the standoff mounting post inside the reflector which impaired the reflected output pattern in that plane.

The intensity gain for any orientation of the reflector was never greater than 1.53. The output pattern was actually less luminous in the central portion of the field (0.48 intensity gain) than it was for the bare flashlamp. The specular reflectivity of the polished surface caused the light output to be concentrated in an annular pattern. The diffuse reflectivity resulting from the irregular surface of the aluminum foil was much more effective than the smooth polished surface. The fact that the source was extended (rather than concentrated at a point which could be placed near the principal focus of the parabola) is one reason that only very poor control of the output beam was possible.

D. PRELIMINARY RANGING

A three-inch retro-reflector was mounted on the fire escape of a nearby building. The distance to this reflector was found by using a theodolite in the lab and measuring the angle defined by two marks placed one foot apart on the fire escape. The distance to the reflector was found to be 391 feet. The expected two-way travel time for the light pulse is 0.785 microseconds.

A strobotac was used as the source. The output of a solar cell placed immediately in front of the source was the oscilloscope's sweep trigger. The waveform detected by a second solar cell also mounted in front of the strobe was displayed on one channel of the CRO. The return pulse was received by Assembly #2 placed alongside the source, and its output was displayed on the other channel of the CRO. (See Fig. 31) The initial pulse was reflected directly back into Assembly #2 to ascertain the "fixed" time delay and jitter of the assembly. Fig. 32 shows an inherent time delay of 0.2 μ sec and jitter approximating 40 nanoseconds were present.

Then the assembly was reoriented to detect the reflected pulse and the results are shown in Fig. 33. The elapsed time totalled 0.9 microseconds. Subtracting the delay inherent in the assembly yields 0.7 microseconds for the actual ranging time. Range error is 83 feet (10.6%). This ranging information was obtained during daylight when fluctuations in the amplitude of the return pulses apparently resulted from thermal currents in the atmosphere.

The reflector was then mounted in the west window of the Bunker Hill Monument. The distance from the south-east point

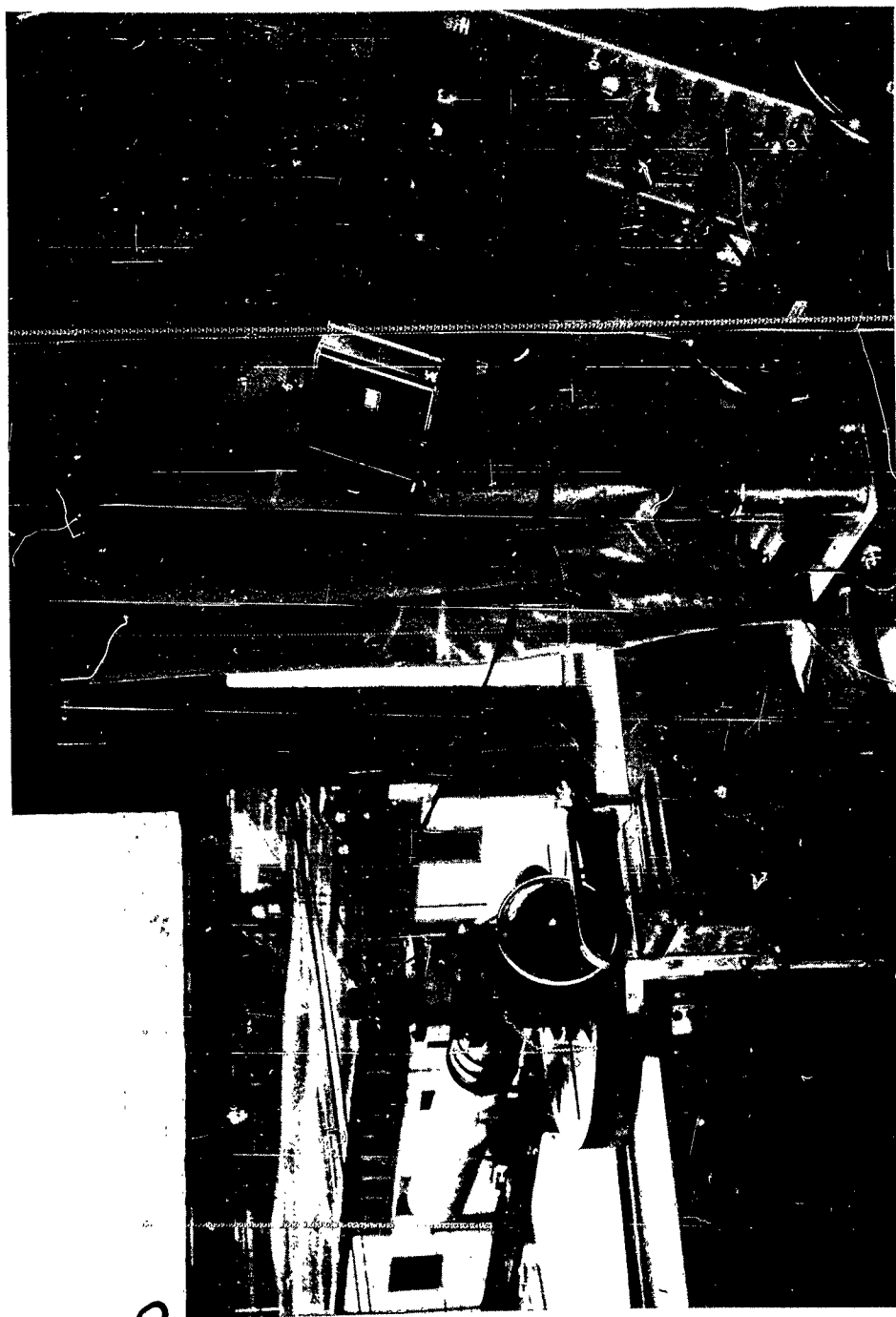
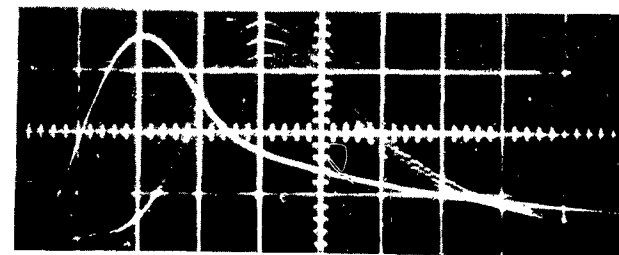


Fig. 31. Ranging to Fire Escape



Sweep rate = 0.2 usec/cm

Fig. 32. Time Delay and Jitter in Assembly #2



Sweep rate = 0.5 usec/cm

Fig. 33. Preliminary Ranging

of the roof of the building at 75 Cambridge Parkway, Cambridge, to the top of the monument was measured by Dr. Max Peterson on December 16th and 17th, 1962, and found to be 5995 feet. Again the strobotac served as the light source and ranging was accomplished from the roof on the evening of May 1st, 1963. The expected travel time for the light pulse was 12.3 μ sec. The measured elapsed time was 12.6 μ sec. Subtracting the inherent delay in the pickup device yields an actual elapsed time of 12.4 μ sec, or only 0.1 μ sec error was present. This is less than 1% error.

CHAPTER IV

CONCLUSIONS AND RECOMMENDATIONS

The application of special design, high-intensity xenon flash beacons for range determination between space vehicles appears to be quite feasible. Preliminary investigation of the most important parameters involved has served to indicate the proper direction for a detailed engineering design of such a ranging device. Specific recommendations include:

- (1) Investigation of the use of a high pressure, xenon filled, three terminal flash-gap which would serve as a combination hold-off device and flashing beacon. It is most important to consider the effect of reduction in battery power during operation which could reduce the applied voltage to the point where the gap would not fire.
- (2) Elimination of the thyratron from the trigger circuit because of the power consumption required to heat the cathode. A simple triggering arrangement is possible using Argon-filled concentric spark gaps. An investigation of the jitter in such an arrangement must be conducted.
- (3) Reduction in overall weight, through the use of light weight components such as high voltage mylar capacitors with very high ringing frequencies, and advanced design DC-DC converters.
- (4) Particular caution exercised in system design to reduce inductance through short leads.
- (5) Modification of the telescope to be used for the Apollo

mission to include a beam splitter to divert half the incoming light flux onto a photocathode surface used in a transponder or timing device.

(6) Consideration of a correlation filter which approximately matches the intensity wave shape to improve the signal-to-noise ratio, or at least a high-pass filter to eliminate low frequency effects of varying background illumination.

(7) Addition of an automatic tracking capability to aid in thrust control.

APPENDIX "A"

The concept of intensity is applicable only when the source of luminous energy is so small that it may be treated as a point. In this report we used the illumination produced by the point source flash-lamp to establish its peak luminous intensity in terms of candlepower. A more correct way of describing the luminous flux produced by a small source would be the luminous intensity of the source needed to radiate dF lumens of flux within a small solid angle $d\omega$. Then the luminous intensity, I , would be measured as $I = dF/d\omega$ in units of candles.

If the source of the luminous flux is too large to be considered a point, the corresponding quantity is brightness. By definition, the brightness in any given direction at any point of the extended surface is the quotient of the intensity of an element of the surface at that point by the area of the element projected in a plane perpendicular to the given direction. In mathematical symbols:

$$B = \frac{dI}{d\sigma \cos \theta}$$

where dI is the intensity of an element of the surface in the specified direction, $d\sigma$ is the area of this element, and θ is the angle between the normal to the surface and the given direction. The unit of brightness is the candle per unit area.

The apparent brightness of an extended surface is independent of the distance at which it is observed; for, as the distance is increased, the total source area covered by the field of view increases by almost exactly the amount to compensate for the decrease in the illumination received from a specified incremental area on the surface.

For this reason we do not need to make any changes in the computed values of brightness for the lunar surface or the "brightness" of the background star field.

When light is incident upon a surface, the resulting illumination is expressed in terms of the amount of flux incident upon a unit area. The unit of illumination is the lumen per square meter for the metric system; the lumen per square foot for the English system. The illumination produced by a point source is given by the well-known inverse-square law, which is

$$E = \frac{I}{d^2} \cos i$$

where I is the intensity of the source, d is its distance from the surface, and i is the angle of incidence measured from the normal to the surface.

For a telescope in which the aperture stop outlining the field of view is circular, the illumination incident on the eye created by the field brightness can be computed by means of the formula, $E = B \omega$, where ω is the solid angle in steradians. When the half-plane angle (θ) is small, the solid angle may be approximated by $\omega = \sin^2 \theta$.³ For the three power telescopes on the space vehicles, $\theta = 10^\circ$ and $\omega = 0.0954$.

APPENDIX B

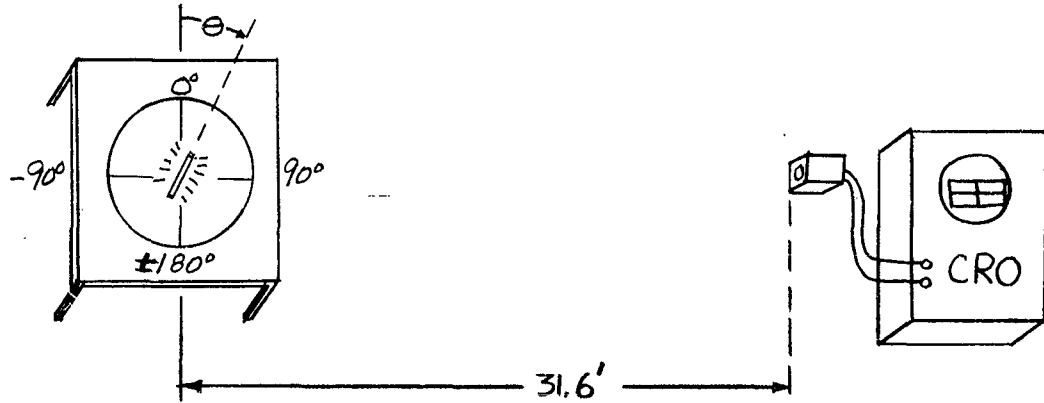
TABLES

TABLE I. INTENSITY AND RISE TIME MEASUREMENTS

Voltage (Kilovolts)	Capacitance (Microfarads)	Input Energy (Joules)	Rise Time (Microseconds)	Peak Intensity (10^6 candlepower)
5.0	0.75	9.38	3.4	7.45
	0.50	6.25	2.8	5.58
	0.25	3.13	2.2	3.14
	0.10	1.25	1.4	2.06
	0.05	0.63	0.6	0.62
10.0	0.75	37.5	3.2	16.1
	0.50	25.0	2.5	13.6
	0.25	12.5	1.7	7.45
	0.10	5.0	0.9	5.00
	0.05	2.5	0.6	2.75
15	0.75	84.4	3.0	27.2
	0.50	56.3	2.4	23.1
	0.25	28.1	1.6	14.5
	0.10	11.3	0.8	9.1
	0.05	5.6	0.6	4.55
20	0.75	150	3.0	43.1
	0.50	100	2.5	31.0
	0.25	50	1.8	20.6
	0.10	20	1.1	12.0
	0.05	10	0.7	6.0

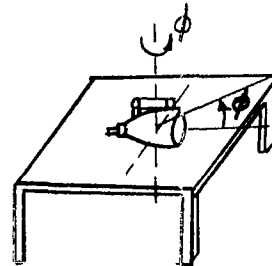
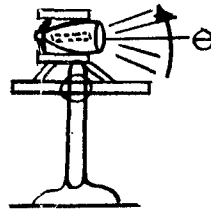
TABLE II. RADIAL DISTRIBUTION OF LUMINOUS FLUX

IN THE HORIZONTAL PLANE



Orientation Angle θ (Degrees)	Peak Intensity (10^6 candlepower)	Normalized Distance Where Illuminations all equal 10^5 lumen- ft^{-2} (Feet)
-90°	1.45	3.81
-75°	14.9	12.20
-60°	20.7	14.38
-45°	24.8	15.74
-30°	27.3	16.50
-15°	28.1	16.75
0°	28.6	16.9
15°	28.1	16.75
30°	27.7	16.63
45°	25.6	16.0
60°	21.5	14.67
75°	14.9	12.20
90°	2.07	4.55

TABLE III. DISTRIBUTION OF LUMINOUS FLUX
FROM PARABOLIC REFLECTOR



Vertical Orientation:

<u>θ</u>	<u>Voltage</u>	<u>Intensity Gain</u>
0°	7.2	.48
5°	9.0	.60
10°	9.5	.634
15°	12.0	.80
20°	13.5	.90
25°	14.5	.966
30°	11.0	.733
35°	8.5	.566
40°	5.2	.347
45°	6.2	.414
50°	5.2	.347
55°	4.8	.32
60°	5.4	.36
65°	4.0	.267

Horizontal Orientation:

<u>θ</u>	<u>Voltage</u>	<u>Intensity Gain</u>
0°	7.2	.48
7.5°	7.2	.48
15°	13.0	.866
22.5°	21	1.4
30°	22	1.47
37.5°	22	1.47
45°	23	1.53
52.5°	16.5	1.1
60°	6.4	.426
67.5°	1.1	.073
75°	0.1	Neg
82.5°	Neg	---

REFERENCES

1. Russell, H. N., Dugan, R. S., and Stewart, J. Q., Astronomy, Volume I, "The Earth as a Planet", Ginn and Company, Boston, 1955, Appendix Table IV.
2. Dole, S. H., Visual Detection of Light Sources On or Near the Moon, USAF Project Rand Research Memorandum, RM-1900, ASTIA Document No. AD133032, 27 May 1957, Page 36.
3. Hardy, A. C. and Perrin, F. H., The Principles of Optics, 1st Ed., Chapter XIX, "The Design of Optical Instruments", McGraw-Hill Book Co., Inc., New York, 1932.
4. Middleton, W. E. K., Vision Through the Atmosphere, Chapter 5, "The Relevant Properties of the Eye", University of Toronto Press, 1952.
5. Blondel, A., and Rey, J., Sur la Perception de Leur Portee, Journal de Phys et le Radium, 1:530-550.
6. Toulimin-Smith, A. K., and Green, H. N., The Fixed Light Equivalent of Flashing Lights, Illuminaion Engineering, (London) Vol. 26, 304-306.
7. Hampton, W. M., "Fixed-Light Equivalent of Flashing Light", Illuminating Engineering, (London) Vol. 27, Pages 46-47.
8. Di Vincenzo, A. P., Constricted Arcs as Pulse Light Sources, S. M. Thesis, Electrical Engineering Department, Massachusetts Institute of Technology, 1947.
9. Mullin, J. J., The Starting Characteristics of Flash Tubes, S. M. Thesis, Department of Electrical Engineering, Massachusetts of Technology, August, 1955.
10. Smith, David, Unpublished Experiments, Department of Electrical Engineering, Massachusetts Institute of Technology, 1963.
11. Loeb, Leonard B. and Meek, John M., The Mechanism of the Spark Gap, Stanford University Press, Stanford University, 1941.
12. Edgerton, H. E. and Shaffner, R., "Transient Light Measurements with Phototubes," Electronics, August 25, 1961, Pages 56-57
13. Martz, E. P., "Visibility: Detection and Recording of Objects Against a Sky Background" Journal of the Society of Motion Picture and Television Engineers, April 1958.

14. Kopal, Zdenek (Ed.), Physics and Astronomy of the Moon, Academic Press, New York, 1962.
15. Summer, W., Photosensors, Chapman and Hall Ltd., London, 1957.
16. Hurlburt, "Brightness and Luminosity of the Night Sky"
Journal of the Optical Society of America, D. S. A. Vol. 37,
1948, Page 1096A.